

IDENTIFICATION OF ALUMINUM TOLERANCE IN THE MODEL LEGUME

MEDICAGO TRUNCATULA

by

YANINA ALARCÓN

(Under the Direction of Wayne Parrott)

ABSTRACT

Acid soils worldwide limit agricultural productivity due to the effect of aluminum (Al) toxicity on plant growth. Al toxicity inhibits root growth and development thus reducing biomass yield in important forage legumes including alfalfa. *Medicago truncatula* is a model legume species with an extensive genomics infrastructure that can facilitate discovery of Al tolerance mechanisms of value for economical important species. The objective of this research was to identify genomic regions relevant to acid and Al tolerance in *M. truncatula* using a recombinant inbred line (RIL) population. The mapping population was obtained from a cross between Mt Core 23 (acid and Al tolerant) and Mt Core 35 (acid and Al sensitive), followed by multiple generations of single seed descent. Genotyping of the F_{4.5} progenies was performed using the Illumina's *Medicago* Golden Gate array with 1,536 single nucleotide polymorphism (SNP) as well as, complementary genotyping of SNPs targeting genomic regions and Al tolerance candidate genes using high resolution melting (HRM) analyses. A whole plant assay was used to evaluate the phenotypic response of the individuals from the RIL population and the parents for root growth at pH 7, pH 4 and pH4 +Al 20 µM. Genomic regions

associated with Al tolerance were detected and the corresponding SNP markers identified. The expression levels of target genes of contrasting genotypes were also evaluated. The practical value of the identified SNPs was evaluated based on their ability to predict the performance of additional RIL individuals when grown under acid and Al toxic conditions. Ultimately, strategies aimed to identify and understand genes and mechanisms of Al tolerance in *Medicago* are relevant and critically needed to deploy breeding strategies in economical important crops including alfalfa.

INDEX WORDS: *Medicago truncatula*, acid soils, aluminum tolerance, QTL, RIL population, SNP, high-resolution melting, alfalfa

IDENTIFICATION OF ALUMINUM TOLERANCE IN THE MODEL LEGUME

MEDICAGO TRUNCATULA

by

YANINA ALARCÓN

BS in Chemistry, Córdoba National University, Argentina, 2007

A Thesis Submitted to the Graduate Faculty of The University of Georgia in Partial

Fulfillment of the Requirements for the Degree

MASTER OF SCIENCE

ATHENS, GEORGIA

2014

© 2014

Yanina Alarcón

All Rights Reserved

IDENTIFICATION OF ALUMINUM TOLERANCE IN THE MODEL LEGUME

MEDICAGO TRUNCATULA

by

YANINA ALARCÓN

Major Professor: Wayne Parrott

Committee: Maria J. Monteros
Alí Missaoui
Miguel A. Cabrera

Electronic Version Approved:

Julie Coffield
Interim Dean of the Graduate School
The University of Georgia
December 2014

DEDICATION

This dissertation is dedicated to my parents Oscar and Cristina and sisters Luciana and Juliana. Also, I want to dedicate this thesis work to my grandparents and friends. They have always been there for me.

ACKNOWLEDGEMENTS

I would like to thank everyone who has support me on my journey during the MS graduate thesis work. Special thanks to Maria Monteros who has encouraged me in everything, since the day I decided to come to UGA to start this process for the MS degree, my M.S. She has always been there for me, supporting my work, encouraging me on my ideas and taking care of me. I have learned many things from her, both for my academic aspirations and my personal life. I also would like to thank Wayne Parrott for admitted me as his student, and helped me navigate this process. I acknowledge Ali Missaoui and Miguel Cabrera for accepting to serve as my committee members and for their advice.

I would also like to thank Christy Motes and Kazuyo Ueda, from the Legume Breeding Lab at the Noble Foundation. They have taught me the lab techniques and lab protocols utilized as part of my research project. Both Christy and Kazuyo gave me a lot of support during the time I spent at Noble and they became great friends. Acknowledgments to Yuanhong Han, Alyssa Nedley and Will Chaney who helped me with my experiments at Noble. Also, I would like to acknowledge Ivonne Torres-Jerez and Stephen Webb who had helped me on the qRT-PCR experiments and statistical analysis, respectively. From UGA, thanks to Jonathan Markham, Joseph, Kurk Lance and all the people who had helped me on any part of my work.

I also would like to thanks all the friends I have gained during my stay at Noble. All of them have a piece of my heart. During my life in Athens, I have met incredible

friends too, like Andrea, Maria, Carolina and Laura and I know we will remind friends forever. I am thankful to have found many people at IPBGG with whom I shared many experiences during classes together and study afternoons and nights. Thanks to all of them, my life was happy and better.

Thanks to the great parents I have. They have encouraged and support me my whole life no matter what, even when I decided to go far from them. Their love was the engine for me to achieve the MS degree and goal of my life as an experience. They are an example to follow for my sisters and me. Luciana, Juliana and my life-friends in Argentina, thank you all for your love.

Finally, I acknowledge The Samuel Roberts Noble Foundation for the financial support for the MS program and to complete the goals for this project.

TABLE OF CONTENTS

	Page
ACKNOWLEDGEMENTS	v
LIST OF TABLES	ix
LIST OF FIGURES	xi
 CHAPTER	
1 INTRODUCTION AND LITERATURE REVIEW	1
Acid soils and aluminum toxicity	1
Aluminum toxicity in plants	2
Mechanisms of aluminum tolerance	3
Translational genomics: models to crops.....	4
Aluminum responses in the model legume <i>Medicago truncatula</i>	6
Aluminum tolerance in the economical important crop alfalfa.....	7
References	9
2 MATERIALS AND METHODS	18
Plant materials.....	18
Phenotyping for acid and aluminum responses	18
Genotyping.....	20
Mapping and QTLs analysis	22
Prediction of RIL phenotypes using SNP markers associated with acid and aluminum QTLs	23

References	24
3 RESULTS AND DISCUSSION	26
Phenotyping for acid and aluminum responses	26
Genotyping.....	27
Mapping and QTLs analysis	28
Prediction of RIL phenotypes using SNP markers associated with acid and aluminum QTLs	31
References.....	34
4 OTHER STRATEGIES TO UNDERSTAND ACID AND ALUMINUM TOLERANCE: GENE EXPRESSION OF STRESS, ACID AND ALUMINUM TOLERANCE CANDIDATE GENES	56
Introduction.....	56
Materials and methods	56
Results and discussion	59
References.....	64
5 CONCLUSION	85

LIST OF TABLES

	Page
Table 3.1: LS-Means procedure of RL ^{0.25} for Treatment ($\alpha = 0.05$)	37
Table 3.2: Covariance parameter estimates for Replication as a random effect in the model RL ^{0.25}	37
Table 3.3: <i>Type III</i> of fixed effects for RL ^{0.25} model ($\alpha = 0.05$).....	37
Table 3.4: <i>Type III</i> of fixed effects for Ratio pH 7 ^{-0.25} model ($\alpha = 0.05$).....	38
Table 3.5: <i>Type III</i> of fixed effects for Ratio pH 4 ^{0.25} model ($\alpha = 0.05$)	38
Table 3.6: Molecular markers associated with RL traits of the <i>M. truncatula</i> RIL population	39
Table 3.7: Genotype prediction of the 5% and 10% top and bottom performing RILs for the trait RL at pH 4. (RL: cm, N: negative HRM amplification reaction, U: unknown genotype class).....	42
Table 3.8: Genotype prediction of the 5% and 10% top and bottom performing RILs for the trait RL at pH 4+ Al 20 μ M. (RL: cm)	43
Table 3.9: Genotype prediction of the 5% and 10% top and bottom performing RILs for the trait RL at pH 4/ RL at pH 7. (N: negative HRM amplification reaction, U: unknown genotype class).....	44
Table 3.10: Genotype prediction of the 5% and 10% top and bottom performing RILs for the trait RL at pH 4+Al 20 μ M/ RL at pH 4. (N: negative HRM amplification reaction, U: unknown genotype class).....	45

Table 3.11: Genotype prediction of the 5% and 10% top and bottom performing RILs for the trait RL at pH 4+Al 20 μ M/ RL at pH 4. (N: negative HRM amplification reaction)	46
Table 4.1: Al response and tolerance candidate genes analyzed by qRT-PCR in the RIL population parental lines Mt Core 23 and Mt Core 35.....	68
Supplementary Table 4.1: Sequences for the forward (PF) and reverse (PR) primers targeting specific transcripts with the unique IMGAG annotations and utilized to evaluate the gene expression of Mt Core 23 and Mt Core 35 using qRT-PCR	70

LIST OF FIGURES

	Page
Figure 2.1: Response to acid and aluminum conditions of the <i>M. truncatula</i> core inbred lines. Mt Core 23 and Mt Core 35 used as parents to generate the RIL population	25
Figure 2.2: Growth and process of inbreeding the <i>M. truncatula</i> RIL population through multiple generations of single seed descent in a greenhouse at the Noble Foundation (Ardmore, OK)	25
Figure 3.1: Phenotype distributions for the RIL mapping population A) RL at pH 7, B) RL at pH 4, C) RL at pH 4+ Al 20 μ M.....	47
Figure 3.2: Phenotype distributions for the RIL mapping population A) RL at pH 4/RL at pH 7, B) RL at pH 4+ Al/ RL at pH 7, C) RL at pH 4+ Al 20 μ M/ RL at pH 4.....	48
Figure 3.3: Conditional residuals for variables of the RL ^{-0.25} phenotypes analyzed with GLIMMIX procedure.....	49
Figure 3.4: Linkage groups obtained and used for mapping Al tolerance genomic regions in the <i>M. truncatula</i> RIL population	50
Figure 3.5: QTLs detected in the <i>M. truncatula</i> RIL population by interval mapping for the different root length (RL) traits A) RL at pH 4, B) RL at pH 4+ Al 20 μ M, C) RL at pH 4/ RL at pH 7, D) RL at pH 4+ Al 20 μ M/ RL at pH7, E) RL at pH 4+	

Al 20 μ M/ RL at pH 4. (The X axis represents cM position and the Y axis the LOD values).....	51
Figure 3.6: QTLs detected in the <i>M. truncatula</i> RIL population by rMQM for the different root length (RL) traits A) RL at pH 4, B) RL at pH 4+ Al 20 μ M, C) RL at pH4/ RL at pH 7, D) RL at pH 4+ Al 20 μ M/ RL at pH7, E) RL at pH 4+Al 20 μ M/ RL pH 4. (The X axis represents cM position and the Y axis the LOD values).....	52
Figure 3.7: QTLs detected in the <i>M. truncatula</i> RIL population by Kruskal-Wallis non-parametric mapping for the different root length (RL) traits A) RL at pH 4, B) RL at pH 4+ Al 20 μ M, C) RL at pH 4/ RL at pH 7, D) RL at pH 4+ Al 20 μ M/ RL at pH 7, E) RL at pH 4+ Al 20 μ M/ RL at pH 4. (The X axis represents the cM position and the Y axis the LOD values).....	53
Figure 3.8: Mean phenotype distributions for the RILs used to predict phenotypes based on markers associated to QTLs for the root length (RL) traits A) RL at pH 4, B) RL at pH 4/ RL at pH 7, C) RL at pH 4+ Al 20 μ M and D) RL at pH 4+Al 20 μ M/ RL at pH 7 E) RL at pH 4+Al 20 μ M/ RL at pH 4.....	55
Figure 4.1: Relative gene expression (fold change) of the dehydrine gene (Medtr7g086340) in root tissues of Mt Core 23 and Mt Core 35. A) Gene expression of the dehydrine gene at pH 4 and pH 4+ Al relative to pH 7, B) Gene expression of the dehydrine gene at pH 4+ Al 20 μ M relative to pH 4.....	72
Figure 4.2: Relative gene expression (fold change) of the dehydrine gene (Medtr7g086340) in leaf tissues of Mt Core 23 and Mt Core 35. A) Gene	

expression of the dehydrine gene at pH 4 and pH 4+Al 20 μ M relative to pH 7, B)
Gene expression of the dehydrine gene at pH 4+ Al 20 μ M relative to
pH 4.....73

Figure 4.3: Relative gene expression (fold change) of the citrate synthase gene
(Medtr5g091930) in root tissues of Mt Core 23 and Mt Core 35. A) Gene
expression of the citrate synthase gene at pH 4 and pH 4+Al 20 μ M relative to
pH 7, B) Gene expression of the citrate synthase gene at pH 4+ Al 20 μ M relative
to pH 4.....74

Figure 4.4: Relative gene expression (fold change) of the citrate synthase gene
(Medtr3g048920) in root tissues of Mt Core 23 and Mt Core 35. A) Gene
expression of the citrate synthase gene at pH 4 and pH 4+Al 20 μ M relative to
pH 7, B) Gene expression of the citrate synthase gene at pH 4+ Al 20 μ M relative
to pH 4.....75

Figure 4.5: Relative gene expression (fold change) of the malate dehydrogenase gene
(Medtr8g1041209) in root tissues of Mt Core 23 and Mt Core 35. A) gene
expression of the malate dehydrogenase gene at pH 4 and pH 4+Al 20 μ M
relative to pH 7, B) Gene expression of the malate dehydrogenase gene at pH 4+
Al 20 μ M relative to pH 4.....76

Figure 4.6: Relative gene expression (fold change) of the citrate transporter gene
(Medtr8g036660) in root tissues of Mt Core 23 and Mt Core 35. A) Gene
expression of the citrate transporter gene at pH 4 and pH 4+ Al 20 μ M relative to
pH 7, B) Gene expression of the citrate transporter gene at pH 4+ Al 20 μ M

relative to pH 4, C) Gene expression of the citrate transporter gene (Medtr7g070210) at pH 4+ Al 20 μ M relative to pH 4.....	77
--	----

Figure 4.7: Relative gene expression (fold change) of the malate transporter gen

(Medtr8g104120) in root tissues of Mt Core 23 and Mt Core 35. A) Gene expression of the malate transporter gene at pH 4 and pH 4+Al 20 μ M relative to pH 7, B) Gene expression of the malate transporter gene at pH 4+ Al 20 μ M relative to pH 4.....	78
--	----

Figure 4.8: Relative gene expression (fold change) of the metal ion binding protein gene

(Medtr7g100450) in root tissues of Mt Core 23 and Mt Core 35. A) Gene expression of the metal ion binding protein gene at pH 4 and pH 4+ Al 20 μ M relative to pH 7, B) Gene expression of the metal ion binding protein gene at pH 4+ Al 20 μ M relative to pH 4.....	79
---	----

Figure 4.9: Relative gene expression (fold change) of the thioredoxin gene

(Medtr2g007340) in root tissues of Mt Core 23 and Mt Core 35. A) Gene expression of the thioredoxin gene at pH 4 and pH 4+ Al 20 μ M relative to pH 7, B) Gene expression of the thioredoxin gene at pH 4+ Al 20 μ M relative to pH 4.....	80
---	----

Figure 4.10: Relative gene expression (fold change) of the peroxidase gene

(Medtr2g029800) in root tissues of Mt Core 23 and Mt Core 35 A) Gene expression of the peroxidase gene at pH 4 and pH 4+ Al 20 μ M relative to pH 7, B) Gene expression of the peroxidase gene at pH 4+ Al 20 μ M relative to pH 4.....	81
--	----

Figure 4.11: Relative gene expression (fold change) of the peroxidase gene (Medtr2g029800) in leaf tissues of Mt Core 23 and Mt Core 35. A) Gene expression of the peroxidase gene at pH 4 and pH 4+Al 20 μ M relative to pH 7, B) Gene expression of the peroxidase gene at pH 4+ Al 20 μ M relative to pH 4.....	82
--	----

Figure 4.12: Relative gene expression (fold change) of the peroxidase gene (Medtr2g029800) in root tissues of Mt Core 23 and Mt Core 35. A) Gene expression of the peroxidase gene at pH 4 and pH 4+Al 20 μ M relative to pH 7, B) Gene expression of the peroxidase gene at pH 4+ Al 20 μ M relative to pH 4.....	83
--	----

Figure 4.13: Relative gene expression (fold change) of the peroxidase gene (Medtr2g029830) in leaf tissues of Mt Core 23 and Mt Core 35. A) Gene expression of the peroxidase gene at pH 4 and pH 4+Al 20 μ M relative to pH 7, B) Gene expression of the peroxidase gene at pH 4+ Al 20 μ M relative to pH 4	84
---	----

CHAPTER 1

INTRODUCTION AND LITERATURE REVIEW

Acid soils and aluminum toxicity

An estimated 30 to 40% of the total arable land worldwide is acidic (von Uexkull and Mutert, 1995). Although the low fertility of acid soils is due to a combination of mineral deficiencies (calcium, magnesium, molybdenum, and phosphorus) and toxicities, toxicity due to aluminum (Al) is the main factor limiting crop production in most acid soils (Eswaran et al., 1997). Al^{3+} is the predominant inorganic monomeric form in the acid soil (Kinraide et al., 1992) and causes severe plant toxicity (Clarkson, 1965; Delhaize and Ryan 1995) resulting in the inhibition of root growth and development (Kochian et al., 2004). Therefore, Al toxicity affects biomass yield and persistence of crops including the forage legume alfalfa (*Medicago sativa* L.) (Graham, 1992; Rechcigl et al., 1988).

Approaches to ameliorate soil acidity and Al toxicity include liming with calcium and magnesium compounds (Barber, 1984). Lime agents include calcite (CaCO_3), dolomite (CaCO_3 , MgCO_3), or a mixture of the two applied to the soil surface (Kochian et al., 2005). However, the application of lime is expensive and only reduces soil acidity of the topsoil layer (Sumner et al., 1986). Therefore, strategies aimed at identifying genetic mechanisms of aluminum tolerance for deployment in breeding programs are relevant and critically needed in crops including forage legume species (Khu et al., 2012).

Aluminum toxicity in plants

Al toxicity inhibits root growth and development and thus limits the ability of the plant to uptake nutrient and water through the root (Kochian et al., 1997). Inhibition of root growth occurs at the root apex (root cap, meristem and elongation zone) and the root hairs as a result of limited cell elongation, expansion and division (Sivaguru and Horst, 1998; Ciamporova, 2002; Frantzios et al., 2001). At the cell wall level, the net negative charge of the cell wall determines its cation exchange capacity (CEC) and thus, the level at which it interacts with the Al ions. The rapid accumulation of Al in the cell wall exerts a damaging effect on root growth in three ways: i) decreased ability of adsorption of basic cations due to the bound Al, thus limiting the plant's ability for nutrient acquisition; ii) the reduced cell expansion limits root elongation and thus affects the capacity for nutrient uptake due to decreased root proliferation in the soil; and iii) adsorption of Al in the cell wall reduces the movement of water and solutes through the apoplast decreasing nutrient uptake by the root (Biamey, 2001, Vardar and Ünal, 2007).

The interactions of Al ions with the plasma membrane can modify its structure thus leading to disturbances of ion-transport processes, which in turn affects cellular homeostasis (Kochian et al., 2005). Also, the Al displacement of calcium (Ca^{2+}) from the membrane surface may increase the apoplastic calcium required to stimulate callose synthesis and its accumulation may produce cellular damage by inhibiting intercellular transport (Sivaguru et al., 2000). In addition, aluminum can significantly inhibit the activity of the plasma membrane H^+ -ATPase, altering the H^+ homeostasis of the root cells (Kochian et al., 2005). Al interactions with signal-transduction pathways, specifically the modification of intracellular Ca^{2+} and pH homeostasis, have been proposed to play

crucial roles in Al toxicity (Ma et al., 2002). Al can also interact with and inhibit the enzyme phospholipase C associated with calcium signaling (Jones and Kochian, 1997). The presence of soluble Al affects the membrane structure due to the generation of reactive oxygen species (ROS) that enhance lipid peroxidation (Cakmak and Horst, 1991).

Al may also disrupt the dynamics of the cytoskeleton thus affecting the process of cell division and cell wall biosynthesis directly by the interaction with microtubules and actin filaments or indirectly, via alteration of signaling cascades such as cytosolic calcium levels (Sivaguru et al., 1999). Al has the capacity to bind to DNA through the nucleoside triphosphates (Grabski and Schindler, 1995), and can therefore affect DNA composition and replication due to the increased rigidity of the double helix and alteration in the chromatin structure (Grabski and Schindler, 1995; Silva et al., 2000).

Mechanisms of aluminum tolerance

Mechanisms of Al tolerance in plants include those that exclude Al from the root apex and those that accumulate Al in the root and shoot symplasm (Kochian et al., 2004). Root Al exclusion mediated by Al-activated organic acid (OA) exudation, such as citrate and malate, from the root apex is the mechanism most studied in crops such as wheat, maize, soybean, sorghum, buckwheat, and rye, among others (Kochian et al., 2005). The exudation of carboxylates anions shortly after exposure of the plant to Al suggests the activation of a carboxylate transporter in the root-cell membrane. Studies in wheat (Ryan et al., 1997; Zhang et al., 2001) and maize (Kollmeier et al., 2001; Piñeros and Kochian, 2001; Piñeros et al., 2002) documented the presence of anion channels as carboxylate

transporters. Alternatively, the mechanism relevant to the accumulation and internal detoxification of Al is accomplished by an Al chelation in the cytosol, followed by the storage of the Al-carboxylate complex in the vacuole (Kochian et al., 2005; Ma et al., 1998; Shen et al., 2002).

Many studies in rice and maize highlight the complex inheritance pattern of Al tolerance (Aniol and Gustafson, 1984; Garvin and Carver, 2003; Giaveno et al., 2001; Luo and Dvorak, 1996; Ma et al., 2002; Magalhaes et al., 2004; Magnavaca et al., 1987; Nguyen et al., 2003, 2001, 2002; Ninamango-Cardenas et al., 2003; Papernik et al., 2001; Reide and Anderson, 1996; Ryan et al., 2009; Shi et al., 2009; Wu et al., 2000). However, in specific populations of certain species only one or two genetic loci account for most of the phenotypic variation (Luo and Dvorak, 1996; Reide and Anderson, 1996; Garvin and Carver, 2003; Ma et al., 2004; Raman et al., 2005; Wang et al., 2007).

Translational genomics: models to crops

Medicago truncatula is a model legume native to the Mediterranean basin. The genus *Medicago* has approximately 54 different characterized species (Lesins and Lesins, 1979). *M. truncatula* has been used as a model species for the study of basic and applied plant research. The natural characteristics that make it a valuable model crop include: diploid and self-fertile species, annual growth habit, short seed-to-seed generation time, relatively small genome size of approximately 500 Mbp (Young and Udvardi, 2009), availability of multiple ecotypes and mutant collections (Ronfort et al., 2006; Tadege et al., 2008), efficient transformation protocols (Trieu and Harrison, 1996; Trinh, et al., 1998; Kamaté et al., 2000), characterized cytogenetics (Cerbah et al., 1999; Kulikova et

al., 2001), and a high quality whole-genome sequence (available at www.medicago.org). Syntenic species share extensive tracts of homologous genes (Ahn and Tanksley, 1993; Gale and Devos, 1998; Devos and Gale, 2000). Because *M. truncatula* and alfalfa are largely syntenic, it was possible to generate a comparative genetic map of them using primers designed from exon sequences to rapidly map genes in *M. sativa* (Choi et al., 2004). Synteny thus enables comparative genomics between species facilitating the use of genomic tools in one species for the discovery of genetic markers and positional gene cloning in another related species (Das et al., 2008; Hougaard et al., 2008; Yang et al., 2008; Han et al., 2011). In addition to the *M. truncatula* genome sequence, the genomes of *Glycine max* L. and *Lotus japonicus* L. provide a solid foundation for comparative genomics with other legumes that have agricultural value including alfalfa (*Medicago sativa* L.), chickpea (*Cicer arietinum* L.), clovers (*Trifolium* sp.), lentil (*Lens* sp.), garden pea (*Pisum sativum* L.) and peanut (*Arachis hypogaea* L.) (Young and Bharti, 2012).

Resources developed and knowledge obtained relevant to patterns of plant growth, development and adaptation to stress responses in model species may be useful for the practical improvement of crop species. For example, the *RCT1* gene which belongs to the family of NBS-LRR disease resistance (R) genes and confers resistance to anthracnose *Colletotrichum trifolii* race 1 (Yang et al., 2007), was identified in *M. truncatula*, map-base cloned and transferred to susceptible alfalfa plants. The result was broad-spectrum anthracnose resistance in previously susceptible alfalfa plants (Yang et al., 2008). This approach has also been useful to address abiotic stress responses in alfalfa. The *WXPI* transcription factor identified in *M. truncatula* confers drought tolerance to transgenic alfalfa plants (Zhang et al., 2005; Jiang et al., 2009).

Aluminum responses in the model legume *Medicago truncatula*

Physiological and molecular characterization of Al responses in *M. truncatula* identified differential expression of genes in response to Al in a set of sensitive and resistant genotypes (Chandran et al., 2008 a). Differential transcript accumulation in the root tips of an Al sensitive genotype during plant growth with and without Al was also evaluated. A total of 2,782 genes with transcript accumulation changes in response to Al were identified and include those associated with organic acid transporters, Ca^{2+} homeostasis regulators, cell wall enzymes, oxidative responses and Al-binding proteins. Of those genes, 324 were up-regulated and 267 genes were down-regulated at least twofold in response to the Al treatment (Chandran et al., 2008 a).

Additional natural genetic variation for Al tolerance was identified in the *M. truncatula* core accessions available at the Germplasm Resources Information Network (GRIN) (Khu et al., 2010). These accessions were included in the re-sequencing efforts of the NSF-funded HapMap project (<http://medicagohapmap.org/>). Briefly, over 300 inbred lines spanning a range in *Medicago* diversity were re-sequenced using Illumina next generation technology to discover single nucleotide polymorphism (SNPs), insertion/deletions (INDELS) and copy number variants (CNV) among the *Medicago* lines. The resulting sequences were used to identify a subset of SNPs distributed throughout the genome that are also polymorphic in a wide range of genotypes. An Illumina's GoldenGate system that includes 1,536 *Medicago* SNPs was generated and is publicly available for genotyping. The Golden Gate technology enables genotyping of the SNPs present in the array of multiple individuals in one reaction (Oliphant et al., 2002), and utilizes allele-specific oligonucleotides (ASOs) to discriminate between the allelic

states at a SNP locus (Fan et al., 2003). The third locus specific oligonucleotide (LSO) primer, anneals downstream of ASO and contains unique sequence for each SNP site. After annealing, the extension and ligation reaction is performed at multiple SNP loci simultaneously. The templates are then PCR amplified with three common SNP sites primers. PCR products are annealed to an array composed of oligonucleotides complementary to sequences in the LSOs that are used for recognition of each SNP site (Gonzalez-Neira et al., 2013) and the ratio of the intensity of fluorescence between dyes is used to determine the allelic state at each SNP site (Akhunov et al., 2009). SNP array genotyping platforms used for SNP genotyping include de Golden gate array, in polyploid wheat (Akhunov et al., 2009) and soybean (Hyten et al., 2008) as well as custom-made arrays used for SNPs genotyping in alfalfa (Li et al., 2014). This technology enables identification of genome-wide associations between loci and agronomical traits of interest (Young and Bharti, 2012).

Aluminum tolerance in the economical important crop alfalfa

Cultivated alfalfa (*Medicago sativa* L.) is an autotetraploid species ($2n = 4x = 32$) (Bingham and Gillies, 1971), and an important perennial forage legume grown worldwide. In the United States alone, 57 million tons of alfalfa hay were produced with a total value exceeding US \$ 10 billion in 2013 alone (http://www.nass.usda.gov/Statistics_by_Subject/). Alfalfa, like the model legume *M. truncatula*, has the capacity for symbiotic nitrogen fixation thus reducing the need for agricultural N fertilizers and is adapted to a range of growing conditions. Productivity and persistence of alfalfa is limited in acid soils because Al toxicity affects root growth

and inhibits nitrogen fixation (Graham, 1992, Rechcigl et al., 1988). The actual management practice to mitigate the acid soil and Al toxicity effects is the addition of lime and fertilizers, but the application cost and inefficacy to ameliorate the subsoil make the practice undesirable.

The natural genetic variability for Al tolerance can be utilized to develop Al tolerant varieties and to explore the function of the genes involved in Al tolerance. Screening efforts in alfalfa to identify germplasm tolerant to acidic conditions have resulted in limited success (Baligar et al., 1989; Bouton, 1996; Dall'Agnol et al., 1996), and thus no Al tolerant alfalfa cultivar is currently commercially available. Efforts to identify genes or QTLs (quantitative trait loci) for Al tolerance in alfalfa began with the identification of Al tolerance in the wild diploid *M. sativa* subsp. *caerulea* (Bouton, 1996). Mapping efforts in diploid alfalfa identified Al tolerance QTL based on a callus bioassay (Sledge et al. 2002; Narasimhamoorthy et al. 2007). Recent studies identified Al tolerance QTL at the tetraploid level (Khu et al., 2013) using a combination of phenotyping approaches (Khu et al., 2012). A whole plant assay (WPA) in media and soil approaches were used to phenotype a population developed from a cross between an Al-tolerant genotype (Altet-4) and an Al-sensitive genotype (NECS-141) (Khu et al., 2012). The traits analyzed from the WPA in media and soil included root length and root dry weight and shoots weight in limed and unlimed soil. The root and shoot dry weight ratios representing the relative growth in unlimed and limed soil (Khu et al., 2012; Khu et al., 2013). Individual Al tolerance QTLs explained between 8 and 35% of the phenotypic variation (Khu et al., 2013). Transgressive segregation was identified for the plant growth traits evaluated and thus both parents likely contributed positive alleles. In soil based

evaluations, multiple QTL were identified associated with dry weight or dry weight ratios, but not all of them were related to Al tolerance (Reyno, 2012). Thus, efforts to identify mechanisms and strategies used in *Medicago* in response to acidic conditions and Al toxicity can be useful to deploy breeding strategies and trait-integration approaches aimed at increasing alfalfa productivity under these conditions.

References

- Akhunov E., C. Nicoletand, and J. Dvorak. 2009. Single nucleotide polymorphism genotyping in polyploid wheat with the Illumina Golden Gate assay. *Theor. Appl. Genet.* 119 (3): 507-17.
- Ahn S. and S.D. Tanksley. 1993. Comparative linkage maps of the rice and maize genomes. *Proc. Natl. Acad. Sci. USA* 90: 7980-84.
- Aniol, A. and J.P. Gustafson. 1984. Chromosome location of genes controlling aluminum tolerance in wheat, rye, and triticale. *Can. J. Genet. Cytol.* 26: 701-705.
- Baligar, V.C., J.H. Elgin, and C.D. Foy. 1989. Variability in alfalfa for growth and mineral uptake and efficiency ratios under aluminum stress. *Agron. J.* 81 (2): 223-229.
- Barber, S.A. 1984. Liming materials and practices, pp. 171–209. *In*: F. Adams (ed.). *Soil acidity and liming*. 2nd ed. Agron. Monogr. 12. ASA, CSSA, Madison, WI.
- Bingham E.T. and C.B. Gillies. 1971. Chromosome pairing fertility and crossing behavior of haploids of tetraploid alfalfa *Medicago sativa* L. *Can J. Genet. Cytol.* 13:195–202.
- Biamey F.P.C. 2001. The role of the root cell wall in aluminum toxicity. *In*: *Plant Nutrient Acquisition: New Perspectives*, eds., N. Ae, Arihara J., Okada K. and Srinivasan A., pp. 201-226. Tokyo, Japan: Springer Verlag.
- Bouton J.H. 1996. Screening the alfalfa collection for acid soil tolerance. *Crop Sci.* 36: 198-200.

- Cakmak I. and W.J. Horst. 1991. Effect of aluminum on lipid peroxidation, Superoxide dismutase, catalase, and peroxidase activities in root tips of soybean (*Glycine max*). *Physiol. Plant.* 83: 463-468.
- Cerbah, M., Z. Kevei, S. Siljak-Yakovlev, E. Kondorosi, and A. Kondor. 1999. FISH chromosome mapping allowing karyotype analysis in *Medicago truncatula* lines jemalong J5 and R-108-1. *Mol. Plant-Microbe Interact.* 12: 947-950.
- Choi, H., D. Kim, T. Uhm, E. Limpens, H. Lim, J. Mun, et al. 2004. A sequence-based genetic map of *Medicago truncatula* and comparison of marker colinearity with *M. sativa*. *Genetics* 166: 1463-1502.
- Clarkson D.T. 1965. The effect of aluminium and some other trivalent metal cations on cell division in the root of *Allium cepa*. *Ann. Bot.* 29: 309-315.
- Ciamporova M. 2002. Morphological and structural responses of plant roots to aluminum at organ, tissue and cellular levels. *Biol. Plant.* 45: 161-171.
- Dall'Agnol M., J.H. Bouton, and Parrott W.A. 1996. Screening methods to develop alfalfa germplasms tolerant of acid, aluminum toxic soils. *Crop Sci.* 36: 64-70.
- Das S., P.R. Bhat, C. Sudhakar, J.D. Ehlers, and S. Wanamaker. 2008. Detection and validation of single feature polymorphisms in cowpea (*Vigna unguiculata* L. Walp) using a soybean genome array. *BMC Genomics* 9:107
- Delhaize E. and P.R. Ryan. 1995. Aluminum toxicity and tolerance in plants. *Plant. Physiol.* 107: 315-321.
- Devos K.M. and M.D. Gale. 2000. Genome relationships: the grass model in current research. *Plant Cell* 12: 637-46.
- Eswaran H, P. Reich and F. Beinroth. 1997. Global distribution of soils with acidity. In: A.C. Moniz, A.M.C. Furlani, R.E. Schaffert, N.K. Fageria, C.A. Rosolem, H. Cantarella, eds, *Plant-soil interaction at low pH: sustainable agriculture and forestry production*. Brazilian Soil Science Society, Campinas, Brazil, pp 159-164.
- Fan J. B., A. Oliphant, R. Shen, B.G. Kermani, F. Garcia, K.L. Gunderson, M. Hansen, F. Steemers, S.L. Butler, P. Deloukas, L. Galver, S. Hunt, C. McBride, M. Bibikova, T. Rubano, J. Chen, E. Wickham, D. Doucet, W. Chang, D. Campbell, B. Zhang, S. Kruglyak, D. Bentley, J. Haas, P. Rigault, L. Zhou, J. Stuelpnagel, and M.S.

- Chee. 2003. Highly parallel SNP genotyping. Cold Spring Harbor Symposium, Quant. Biol. 68:69-78.
- Frantzios G., B. Galatis B, and P. Apostolakos. 2001. Aluminum effects on microtubule organization in dividing root tip cells of *Triticum turgidum*. II. Cytokinetic cells. J Plant Res. 114: 157-170.
- Gale M.D. and K.M. Devos. 1998. Comparative genetics in the grasses. Proc. Natl. Acad. Sci. USA 95: 1971-7.
- Garvin D.F. and B.F. Carver. 2003. Role of the genotype in tolerance to acidity and aluminum toxicity. *In*: Handbook of soil acidity, eds., Z. Rengel pp. 387-406.
- Giaveno G.D., F.J.B. Miranda, and P.R Furlani. 2001. Inheritance of aluminum tolerance in maize (*Zea mays L.*). J. Gen. Breed. 55:51-56.
- Gonzalez-Neira, A. 2013. The Golden Gate genotyping assay: Custom design, processing and data analysis. Pharmacogenomics. Methods in Molecular Biology. 1015:147-153.
- Grabski S. and M. Schindler. 1995. Aluminum induces rigor within the actin network of soybean cells. Plant Physiol. 108: 897-901.
- Graham, P.H. 1992. Stress tolerance in *Rhizobium* and *Bradyrhizobium*, and nodulation under adverse soil conditions. Can. J. Microbiol. 38:475-484.
- Han Y., Y. Kang, I. Torres-Jerez, F. Cheung, and C.D. Town. 2011. Genome-wide SNP discovery in tetraploid alfalfa using 454 sequencing and high resolution melting analysis. BMC Genomics 12:350.
- Hougaard B.K., L.H. Madsen, N. Sandal, M. de Carvalho Moretzsohn, J. Fredslund, L. Schauser, A.M. Nielsen, T. Rhode, S. Sato, S. Tabata, D.J. Bertioli, and J. Stougaard. 2008. Legume anchor markers link syntenic regions between *Phaseolus vulgaris*, *Lotus japonicus*, *Medicago truncatula* and *Arachis*. Genetics 179:2299-312.
- Hyten, D., Q. Song, I.- Y. Choi, M.-S. Yoon, J. Specht, L. Matukumalli, R.L. Nelson R.C. Schoemaker, N.D. Young, P.B. Cregan. 2008. High-throughput genotyping with the GoldenGate assay in the complex genome of soybean. Theoret. Appl. Genet. 116:945-952.

- Hyten, D., S. Cannon, Q. Song, N. Weeks, E. Fickus, R. Shoemaker, J.E. Specht, A.D. Farmer, G.D. May, and P.B. Cregan. 2010. High-throughput SNP discovery through deep resequencing of a reduced representation library to anchor and orient scaffolds in the soybean whole genome sequence. *BMC Genomics* 11:38.
- Jiang, Q., J.Y. Zhang, X. Guo, M.J. Monteros, and Z.Y. Wang. 2009. Physiological characterization of transgenic alfalfa (*Medicago sativa*) plants for improved drought tolerance. *International Journal of Plant Sciences* 170:969-978.
- Jones D.L. and L.V. Kochian. 1997. Aluminum interaction with plasma membrane lipids and enzyme metal binding sites and its potential role in Al cytotoxicity. *FEBS Letters* 400:51-57.
- Kamaté, K., I.D. Rodriguez-Llorente, M. Scholte, P. Durand, and P. Ratet. 2000. Transformation of floral organs with GFP in *Medicago truncatula*. *Plant Cell Rep.* 19:647-653.
- Kerven G.L., D.G. Edwards, C.J. Asher, P.S. Hallman, and S. Kobot. 1989. Aluminium determination in soil solution. I. Evaluation of existing colorimetric and separation methods for the determination of inorganic monomeric aluminium in the presence of organic acid ligands. *Aust. J. Soil Res.* 27:79-90.
- Khu, D.M., Y. Han, C.M. Motes, and M.J. Monteros. 2010. Aluminum tolerance in a *Medicago truncatula* core collection. Vth International Conference on Legume Genomics and Genetics. July 2-8. Asilomar, CA.
- Khu, D.-M., R. Reyno, E.C. Brummer, and M.J. Monteros. 2012. Screening methods for aluminum tolerance in alfalfa. *Crop Sci.* 52:161-167.
- Khu D.-M., R. Reyno, Y. Han, P.X. Zhao, J.H. Bouton, E.C. Brummer, and M.J. Monteros. 2013. Identification of aluminum tolerance quantitative trait loci in tetraploid alfalfa. *Crop Sci.* 53:148-163.
- Kinraide T.B., P.R. Ryan, and L.V. Kochian. 1992. Interactive effects of Al^{3+} , H^{+} , and other cations on root elongation considered in terms of cell-surface electrical potential. *Plant Physiol.* 99:1461-1468.
- Kochian L.V. and D.L. Jones. 1997. Aluminum toxicity and resistance in plants. In *Research Issues in Aluminum Toxicity*, ed. R Yokel, MS Golub, pp. 69-90. Washington, DC: Taylor and Francis.

- Kochian L.V., O.A. Hoekenga, and M.A. Piñeros. 2004. How do crop plants tolerate acid soils? Mechanisms of aluminum tolerance and phosphorous efficiency. *Annu. Rev. Plant. Biol.* 55:459-493.
- Kochian L.V., M.A. Piñeros, and O.A. Hoekenga. 2005. The physiology, genetics and molecular biology of plant aluminum resistance and toxicity *Plant Soil.* 274:175-195.
- Kollmeier M., P. Dietrich, C.S. Bauer, W.J. Horst, and R. Hedrich. 2001. Aluminum activates a citrate-permeable anion channel in the aluminum-sensitive zone of the maize root apex. A comparison between an aluminum-sensitive and an aluminum resistant cultivar. *Plant Physiol.* 126:397-410.
- Kulikova, O., G. Gualtieri, R. Geurts, D. Kim, D. Cook, T. Huguet, J.H. de Jong, P.F. Fransz, and T. Bisseling. 2001. Integration of the FISH pachytene and genetic maps of *Medicago truncatula*. *Plant J.* 27:49-58.
- Lesins, K. A. and I. Lesins. 1979 Genus *Medicago* (*Leguminoase*): A taxogenetic study. Dr. W. Junk by publishers, The Hague.
- Li, X., A. Acharya, A.D. Farmer, J.A. Crow, A.K. Bharti, R.S. Kramer, Y. Wei, Y. Han, J. Gou, G.D. May, M.J. Monteros, and E.C. Brummer. 2012. Prevalence of single nucleotide polymorphism among 27 diverse alfalfa genotypes as assessed by transcriptome sequencing. *BMC Genomics* 13:568.
- Li, X., Han Y., Wei Y., Acharya A., Farmer A.D., et al. 2014 Development of an Alfalfa SNP Array and its use to evaluate patterns of population structure and linkage disequilibrium. *PLoS ONE* 9 (1): e84329. doi: 10.1371/journal.pone.0084329
- Luo M.-C. and J. Dvořák. 1996. Molecular mapping of an aluminum tolerance locus on chromosome 4D of Chinese Spring wheat. *Euphytica* 91:31-35.
- Ma Z. and S.C. Miyasaka. 1998. Oxalate exudation by *taro* in response to Al. *Plant Physiol.* 118:861-65.
- Ma J.F., S. Nagao, K. Sato, H. Ito, J. Furukawa, and K. Takeda. 2004. Molecular mapping of a gene responsible for Al-activated secretion of citrate in barley. *J. Exp. Bot.* 55:1335-1341.

- Ma J.F., Z. Rengel, and J. Kuo. 2002. Aluminum toxicity in rye (*Sécale céréale*). Root growth and dynamics of cytoplasmic Ca^{2+} in intact root tips. *Ann. Bot.* 89: 241-244.
- Magalhaes J.V., D.F. Garvin, Y.H. Wang, M.E. Sorrells, P.E. Klein, R.E. Schaffert, L. Li, and L.V. Kochian. 2004. Comparative mapping of a major aluminum tolerance gene in sorghum and other species in the *Poaceae*. *Genetics* 167:1905-1914.
- Magnavaca R., C.O. Gardner, and R.B. Clark. 1987. Inheritance of aluminum tolerance in maize. In *Genetic Aspects of Plant Mineral Nutrition*, ed. HW Gabelman, BC Loughman, pp. 201-212. Dordrecht, The Neth: Martinus Nijhoff.
- Manly, K.F., R.H. Cudmore, and J.M. Meer. 2001. Map Manager QTX, cross-platform software for genetic mapping. *Mammal. Genome* 12:930-932.
- Nguyen B.D, D.S. Brar, B. C. Bui, T. V. Nguyen, L.N. Pham, and H.T. Nguyen. 2003. Identification and mapping of the QTL for aluminum tolerance introgressed from the new source, *Oryza rufipogon* Griff., into indica rice (*Oryza sativa* L.). *Theor. Appl. Genet.* 106:583-93.
- Nguyen V.T., M.D. Burow, H.T. Nguyen, B.T. Le, T.D. Le, and A.H. Paterson. 2001. Molecular mapping of genes conferring aluminum tolerance in rice (*Oryza sativa* L.). *Theor. Appl. Genet.* 102:1002-10.
- Nguyen V.T., B.D. Nguyen, S. Sarkarung, C. Martinez, A.H. Paterson, and H.T. Nguyen. 2002. Mapping of genes controlling aluminum tolerance in rice: comparison of different genetic backgrounds. *Mol. Genet. Genomics* 267:772-80.
- Ninamango C.F.E., C.T. Guimaraes, P.R. Martins, S.N. Parentoni, and N.P. Carneiro. 2003. Mapping QTLs for aluminum tolerance in maize. *Euphytica* 130: 223-32.
- Papernik L.A, A.S. Bethea., T.E. Singleton, J.V. Magalhaes, D.F. Garvin, and L.V. Kochian. 2001. Physiological basis of reduced Al tolerance in di-telosomic lines of Chinese Spring wheat. *Planta* 212:829-34.
- Piñeros M.A. and L.V. Kochian. 2001. A patchclamp study on the physiology of aluminum toxicity and aluminum tolerance in maize, identification and characterization of *Al3C* induced anion channels. *Plant Physiol.* 125:292-305.

- Piñeros M.A., J.V. Magalhaes, V.M.C. Alves, and L.V. Kochian. 2002. The physiology and biophysics of an aluminum tolerance mechanism based on root citrate exudation in maize. *Plant Physiol.* 129:1194-206.
- Radovic, J., D. Sokolovic, and J. Markovic'. 2009. Alfalfa-most important perennial forage legume in animal husbandry. *Biotechnology in Animal Husbandry* 25:465-475.
- Raman H., K.R. Zhang., M. Cakir, R. Appels, D.F. Garvin, L.G. Maron, L.V. Kochian, J.S. Moroni, R. Raman, M. Imtiaz, et al. 2005. Molecular characterization and mapping of ALMT1, the aluminium-tolerance gene of bread wheat (*Triticum aestivum* L.). *Genome* 48:781-791.
- Reyno Podesta, R.A. 2012. Improving acid and aluminum tolerance in alfalfa using breeding and genomics. Available from: U of Georgia Catalog, Ipswich, MA.
- Rechcigl, J.E., R.B. Reneau, Jr., and L.W. Zelazny. 1988. Soil solution Al as a measure of Al toxicity to alfalfa in acid soils. *Commun. Soil Sci. Plant. Anal.* 19:989-1001.
- Reide C.R. and J.A. Anderson. 1996. Linkage of RFLP markers to an aluminum tolerance gene in wheat. *Crop Sci.* 36:905-909.
- Ronfort, J., T. Bataillon, S. Santoni, M. Delalande, J. David, and J.-M. Prosper. 2006. Microsatellite diversity and broad scale geographic structure in a model legume: building a set of nested core collection for studying naturally occurring variation in *Medicago truncatula*. *BMC Plant Biology* 6:28.
- Ryan, P.R., M. Skerrett, G.P. Findlay, E. Delhaize, and S.D. Tyerman. 1997. Aluminum activates an anion channel in the apical cells of wheat roots. *Proc. Nat. Acad. Sci.* 94:6547-6552.
- Ryan P.R., H. Raman, S. Gupta, W.J. Horst, and E. Delhaize. 2009. A second mechanism for aluminum resistance in wheat relies on the constitutive efflux of citrate from roots. *Plant Physiol.* 149:340-351.
- Sawaki, Y., S. Iuchi, Y. Kobayashi, Y. Kobayashi, T. Ikka, N. Sakurai, et al. 2009. *STOP1* regulates multiple genes that protect *Arabidopsis* from proton and Aluminum toxicities. *Plant. Physiol.* 150:281-294.
- Shen R., J.F. Ma, M. Kyo, and T. Iwashita. 2002. Compartmentation of aluminium in leaves of an Al-accumulator, *Fagopyrum esculentum* Moench. *Planta* 215:394-98.

- Shi B.J., J.P. Gustafson, J. Button, J. Miyazaki, M. Pallotta, N. Gustafson, H. Zhou, P. Langridge, and N.C. Collins. 2009. Physical analysis of the complex rye (*Secale cereale* L.) *Alt4* aluminium (aluminum) tolerance locus using a whole-genome BAC library of rye cv. Blanco. *Theoret. Appl. Genet.* 119:695-704.
- Silva I., T. Smyth, D. Moxley, T. Carter, N. Allen, and T. Rufty. 2000. Aluminum accumulation at nuclei of cells in the root tip. Fluorescence detection using lumogallion and confocal laser scanning microscopy. *Plant Physiol.* 123:543-552.
- Sivaguru M., T. Fujiwara, J. Samaj, F. Baluska, Z. Yang, H. Osawa, T. Maeda, T. Mori, D. Wolkman, and H. Matsumoto. 2000. Aluminum induced 1-3|-i-D-glucan inhibits cell-to-cell trafficking of molecules through plasmodesmata. A new mechanism of aluminum toxicity in plants. *Plant Physiol.* 124:991-1006.
- Sivaguru M., F. Baluska, D. Volkman, H.H. Felle, and W.J. Horst. 1999. Impacts of aluminum on the cytoskeleton of the maize root apex. Short term effects on the distal part of the transition zone. *Plant Physiol.* 119:1073-1082.
- Sivaguru M. and W.J. Horst. 1998. The distal part of the transition zone is the most aluminum sensitive apical root zone of maize. *Plant Physiol.* 116:155-163.
- Sledge M.K., J.H. Bouton, M. Dall'Agnoll, W.A. Parrott, and G. Kochert. 2002. Identification and confirmation of aluminum tolerance QTL in diploid *Medicago sativa* subsp. *coerulea*. *Crop Sci.* 42:1121-1128.
- Sledge M., I. Ray, and G. Jiang. 2005. An expressed sequence tag SSR map of tetraploid alfalfa (*Medicago sativa* L.). *Theor Appl Genet* 111:980-992.
- Sumner M.E., H. Shahandeh, J. Bouton, and J. Hammel. 1986. Amelioration of an acid soil profile through deep liming and surface. *Soil Sci. Soc. Am. J.* 50:1254-1258.
- Tadege, M., J. Wen, J. He, H. Tu, Y. Kwak, and A. Eschstruth, A. Cayrel, G. Endre, P.X. Zhao, M. Chabaud, P. Ratet, and K.S. Mysore. 2008. Large-scale insertional mutagenesis using the Tnt1 retrotransposon in the model legume *Medicago truncatula*. *Plant J.* 54:335-347.
- Trieu, A.T. and M. J. Harrison. 1996. Rapid transformation of *Medicago truncatula* regeneration via shoot organogenesis. *Plant Cell Rep.* 16:6-11.
- Trinh T., P. Patel, E. Kondorosi, P. Durand, K. Kamate, P. Baner, A. Kondorosi. 1998. *Plant Cell Rep.* 17:345-355.

- von Uexküll H.R. and E. Mutert. 1995. Global extent, development and economic impact of acid soils. *Plant Soil* 171: 1-15.
- Wang J.P., H. Raman, M.X. Zhou, P.R. Ryan, E. Delhaize, D.M. Hebb, N. Coombes, and N. Mendham. 2007. High-resolution mapping of the *Alp* locus and identification of a candidate gene *HvMATE* controlling aluminium tolerance in barley (*Hordeum vulgare* L.). *Theor. Appl. Genet.* 115:265-276.
- Wu P., C. Y. Liao, B. Hu, K.K. Yi, W.Z. Jin, J.J. Ni, and C. He. 2000. QTLs and epistasis for aluminum tolerance in rice (*Oryza sativa* L.) at different seedling stages. *Theor. Appl. Genet.* 100:1295-303.
- Yang, S., M. Gao, S. Deshpande, S. Lin, B. Roe, and H. Zhu. 2007. Genetic and physical localization of an anthracnose resistance gene in *Medicago truncatula*. *Theoret. Appl. Genet.* 116:45-52.
- Yang S, M. Gao, C. Xu, J. Gao, S. Deshpande, S. Lin, B.A. Roe, and H. Zhu. 2008. Alfalfa benefits from *Medicago truncatula*: the RCT1 gene from *M. truncatula* confers broad-spectrum resistance to anthracnose in alfalfa. *Proc. Natl. Acad. Sci. USA* 105:12164-69
- Young N.D. and M. Udvardi. 2009. Translating *Medicago truncatula* genomics to crop legumes. *Curr. Opin. Plant. Biol.* 12:193-201.
- Young, N.D. and A.K. Bharti. 2012. Genome-Enabled Insights into Legume Biology. *Ann. Rev. Plant. Biol.* 63:283-305.
- Zhang W.H., P.R. Ryan, and S.D. Tyerman. 2001. Malate-permeable channels and cation channels activated by aluminum in the apical cells of wheat roots. *Plant. Physiol.* 125:1459-72.
- Zhang, J.-Y., C.D. Broeckling, E.B. Blancaflor, M.K. Sledge, L.W. Sumner, and Z.-Y. Wang. 2005. Overexpression of *WXP1*, a putative *Medicago truncatula* AP2 domain-containing transcription factor gene, increases cuticular wax accumulation and enhances drought tolerance in transgenic alfalfa (*Medicago sativa*). *Plant J.* 42:689-707.

CHAPTER 2

MATERIALS AND METHODS

Plant materials

The *M. truncatula* accessions from the core collection capturing the genetic diversity at the sampled loci were evaluated for their performance and root growth in acid and Al-toxic conditions using a whole plant assay (Khu et al., 2012). The accessions Mt Core 23 (PI493297, Portugal) and Mt Core 35 (PI577611, Germany) showed contrasting performance for both acid and Al tolerance responses (Fig. 2.1) and thus were used as parental genotypes. A total of 1,056 progenies resulting from the cross between Mt Core 23 \times Mt Core 35 were inbred in a greenhouse in Ardmore, Oklahoma (Fig. 2.2) through single seed descent (SSD) to generate the F_{4:5} *M. truncatula* population of recombinant inbred lines (RILs).

Phenotyping for acid and aluminum responses

A subset of 384 *M. truncatula* F_{4:5} RILs were evaluated for acid and Al and tolerance using the whole plant assay (WPA) previously described in Khu et al., 2012. Based on these results, 180 lines covering the range of Al phenotypic responses based on root growth were identified and together with the parental genotypes were grown under three different treatments as variants of the CaCl₂ method: pH 7, pH 4, pH 4 +Al 20 μ M as previously described (Khu et al., 2012) with slight modifications. In this experiment, the pH of the Ca7 media was adjusted to 10.6 and the pH of both the Ca4 and CaAl20 μ M media adjusted to pH 2.4 prior to autoclaving.

Pods from each of the selected RIL lines and the parents were processed to clean the seeds and a scarification process in acid was done to germinate seed in Petri dishes. Scarified seeds were then soaked for 10 min in sulfuric acid and then rinsed 5 times with sterile MiliQ water. After that, seeds were soaked for 10 min in a solution with commercial bleach (20% bleach, 80% water and few drops of Tween 20). The seeds were rinsed three times with sterilized MiliQ water and later placed in Petri dishes with a MS salt media. The MS salt media at a final pH of 5.8 contains 1.125 g Murashige and Skoog Basal Medium with Vitamins, (Phytotechnologies Lab M519), 5 g of sucrose (Ultrapure Sucrose, Invitrogen, 15503-022), 4 g of agar (Agar Micropropagation, Type I, Caisson A038), and 100 uL of PPM solution (Preservative for Plant Tissue Culture Media, Plant Cell Technology). Finally, Petri dishes were placed at 4°C for 48 h and then transferred to a growth chamber for 24 h.

Young uniform seedlings of 3 d old plants were transferred to the WPA treatment media tubes (pH 7, pH 4 and pH 4+Al 20 μ M). The experimental design included three biological replications in a randomized complete design placed in the Conviron CMP 4030 growth chamber set at 24°C, a photoperiod of 18 h and a light intensity of 100 μ mol. After 14 d of growth (Reps 1 to 2) and 15 d of growth (Rep 3), plant roots were scanned using an Epson Perfection V33 scanner and resulting images analyzed for root growth (root length) using the WinRHIZO software (Regent Instrument Inc., Quebec, Canada). Statistical analysis for significance of root length was performed using Generalized Linear Mixed Model (GLIMMIX) with Replicate set as a random effect with SAS 9.3 (SAS Institute Inc., Cary, NC, USA). The six traits analyzed included: 1) Root length at pH 7 (RL at pH 7), 2) Root length at pH 4 (RL at pH 4), 3) Root length at pH 4+

Al 20 μ M (RL at pH 4+ Al 20 μ M), 4) Ratio of root length at pH 4/ RL at pH 7 (RL at pH 4/ RL at pH7), 5) Ratio of root length at pH 4+ Al 20 μ M/ Root length at pH 7 (RL at pH4+ Al 20 μ M/ RL at pH7, and 6) Root length at pH 4+ Al 20 μ M/ Root length at pH 4 (RL at pH4 Al 20 μ M/ RL at pH 4). The RL ratios of RL at pH 4/ RL at pH 7 and RL at pH 4+ Al 20 μ M/ RL at pH 7 provide an estimate of the relative growth of the acid and Al treatments compared to pH neutral conditions (RL at pH 7). The ratio RL at pH4+ Al 20 μ M/ RL at pH 4 captures growth in the presence of Al compared to acidic pH (RL at pH 4) without Al.

Genotyping

A subset of 178 *M. truncatula* F_{4:5} RILs contrasting for their acid and Al tolerance response and the two parental genotypes (total of 180 samples) were genotyped using the custom *Medicago* OPA reagents and Illumina's GoldenGate Genotyping platform at the BioMedical Genomics Center (BMGC) at the University of Minnesota (UMN). Prior to genotyping these *M. truncatula* RILs, a set of 96 *M. truncatula* samples included in the HapMap re-sequencing effort were used for quality testing of the OPAs to compare the GoldenGate results with the known sequences (performed in Dr. Nevin Young's laboratory at UMN). DNA from the *M. truncatula* RILs was extracted using Promega Wizard[®] Genomic DNA Purification kit and quantified with Promega PicoGreen[®] dsDNA kit (Promega, Madison, WI, USA). A normalized 250 ng of DNA was processed using Illumina's GoldenGate chemistry with binding of assay-specific oligos to the cDNA. These are extended and ligated, followed by PCR amplification and hybridization of the beadchip overnight. The beadchip was washed and scanned using Illumina's iScan

instrument (Illumina Inc., San Diego, CA, USA). The software Illumina's GenomeStudio™ version (Illumina Inc., San Diego, CA, USA) was used to analyze and visualize the genotyping results. Following standard recommendations from the laboratory performing the genotyping, all SNPs with a call frequency below 0.9 were turned off as well as samples with a call rate below 0.9 to ensure the use of only high quality SNP calls. The average call rate was 98.0% and the average GenTrain Score was 0.59. As a complement to the genotyping approach described above, SNPs targeting candidate genes relevant to Al tolerance were also tested for polymorphisms between the parents initially, followed by genotyping the polymorphic ones in the RIL population. The *M. truncatula* Gene Index (MtGI) release 10.0 maintained by the Dana Farber Cancer Institute (<http://compbio.dfci.harvard.edu/cgi-bin/tgi/gimain.pl?gudb=medicago> [accessed 15 Oct.2009]) was used to identify current TC sequences from genes differentially expressed in response to Al tolerance stress (Chandran et al., 2008a; Chandran et al., 2008b; Khu et al., 2013). A total of 498 SNP primers targeting these Al candidate genes (Khu et al., 2013) and other genes differentially expressed in response to Al (Tsutsui et al., 2012) were evaluated for polymorphism between the parents Mt Core 23 and Mt Core 35 using the high-resolution melting approach previously described (Han et al., 2012). Criteria used for primer design included a predicted annealing temperature (T_m) of 59°C to 61°C, primer length between 18 and 24 bp, PCR amplicon lengths of 100 to 150 bp and limited self-complementary and poly-X (Han et al., 2012). DNA from the two parental lines was extracted from young leaves with Promega Wizard® Genomic DNA Purification kit (Promega, Madison, WI, USA) and quantified using NanoDrop ND-1000 (Thermo Fisher Scientific Inc., Wilmington, DE, USA). All the PCR reactions

were performed in 384 well plates using Gene Amp PCR system 9700 (Applied Biosystems, Foster City, CA, USA) thermocyclers. The PCR reaction mix consisted of 5 ng of genomic DNA, 0.25 μ M of the forward and reverse SNP primers, 1 X LightScanner High Sensitivity Master Mix (Idaho Technologies, Inc) and 10 μ L of mineral oil. The PCR program includes an initial denaturation step of 2 min at 94°C, 40 PCR cycles with 30 s of denaturation at 94°C and 30 s at 65°C (annealing temperature), followed by a final hold at 4°C (Han et al., 2011). SNPs were assayed using high-resolution melting (HRM) analysis implemented in the Light Scanner HRI 384 (Idaho Technology, Inc., Salt Lake City, Utah, USA). SNP calls were determined using the LightScanner Software CALL-IT 2.0 (Idaho Technology Inc., Salt Lake City, Utah, USA) as previously described (Han et al., 2012). Polymorphic SNPs were genotyped in the first set of 180 RIL (mapping set) and the parents exactly as previously described.

Mapping and QTL analysis

Polymorphic SNP markers from the Illumina's Golden Gate array and from Al tolerance candidate genes were mapped using the Kosambi mapping function implemented in JoinMap[®] 4.1 software (van Ooijen and Voorrips, 2001). Linkage groups were generated based on regression mapping and recombination frequencies.

Based on preliminary linkage groups analysis, 322 additional random SNPs were screened for polymorphisms on the parental lines to cover gaps in markers coverage.

QTL analysis was performed for the six phenotypic traits (RL at pH 7, RL at pH 4, RL at pH 4+ Al 20 μ M, RL at pH 4/ RL at pH 7, RL at pH 4+ Al 20 μ M/ RL at pH 7 and RL at pH 4+ Al 20 μ M/ RL at pH 4) separately using the same genotyping data.

MapQTL[®] 6 (Van Ooijen, 2009) was used to map QTLs for each RL traits using the interval Mapping, restrictive composite interval mapping (rMQM) and Kruskal-Wallis mapping functions.

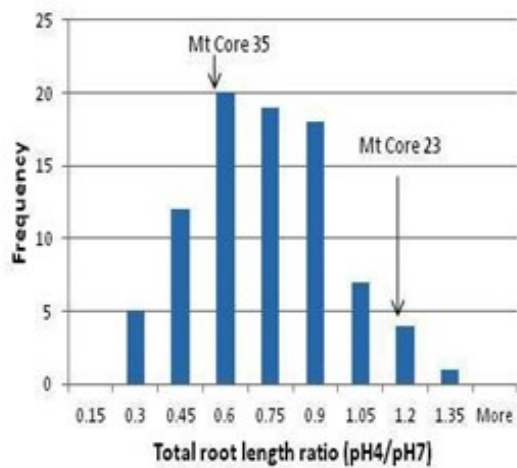
Prediction of RIL phenotypes using SNP markers associated with acid and aluminum QTLs

The results from the initial WPA screening of 384 *M. truncatula* lines were used to identify 130 additional plants to test the hypothesis that molecular markers associated with Al tolerance identified from the first set of RILs could be used to predict the response to Al of some of the remaining RILs (validation set). Phenotypic data for five traits (RL at pH 4, RL at pH 4+ Al 20 μ M, RL at pH 4/ RL at pH 7, RL at pH 4+ Al 20 μ M/ RL at pH 7, and RL at pH 4+ Al 20 μ M/ RL at pH 4) were analyzed for overall mean performance and represented on a histogram to evaluate the normal distribution of the phenotypic data. The top and bottom 5% and 10% performers for each trait were identified and DNA of these RILs was extracted as previously described. PCR and HRM analysis were performed with the 19 SNPs primers flanking the acid and Al tolerance QTLs identified in this study. These included 17 SNPs from the array, for which individual primers were synthesized for additional genotyping of the validation set of RILs using the HRM platform, and five SNPs obtained from Al candidate genes. Primers targeting SNPs from the array were designed with Primer3 software (Rozen and Skaletsky, 1998) following the same parameters for primer design as previously described.

References

- Chandran, D., N. Sharopova, S. Ivashuta, J. Gantt, K. Vandenbosch, and D. Samac. 2008a. Transcriptome profiling identified novel genes associated with aluminum toxicity, resistance and tolerance in *Medicago truncatula*. *Planta*, 228 (1):151-166.
- Chandran D., N. Sharopova, K. VandenBosch, D.F. Garvin, and D.A. Samac. 2008b. Physiological and molecular characterization of aluminum resistance in *Medicago truncatula*. *BMC Plant Biology* 8:89.
- Han, Y., D.M. Khu, M.J. Monteros. 2012. High resolution melting analysis for SNP genotyping and mapping in tetraploid alfalfa (*Medicago sativa* L.). *Molecular Breeding* 29:489-501.
- Khu, D.-M., R. Reyno, E.C. Brummer and M.J. Monteros. 2012. Screening methods for aluminum tolerance in alfalfa. *Crop Sci.* 52:161-167.
- Khu D.-M., R. Reyno, Y. Han, P.X. Zhao, J.H. Bouton, E.C. Brummer, and M.J. Monteros. 2013. Identification of aluminum tolerance quantitative trait loci in tetraploid alfalfa. *Crop Sci.* 53:148-163.
- Kosambi, D.D. 1944. The estimation of map distances from recombination values. *Ann. Eugen.* 12:172-175.
- Oliphant A., D.L. Barker, J.R. Stuelpnagel and M.S. Chee. 2002. BeadArray technology: enabling an accurate, cost-effective approach to highthroughput genotyping. *Biotechniques Suppl.* 5:6-58.
- Untergrasser A, I. Cutcutache, T. Koressaar, J. Ye, B.C. Faircloth, M. Remm, and S. G. Rozen. 2012. Primer3- new capabilities and interfaces. *Nucleic Acids Research* 40(15):e115
- Tsutsui, T., N. Yamaji, C.F. Huang, R. Motoyama, Y. Nagamura, and J.F. Ma. 2012. Comparative genome-wide transcriptional analysis of Al-responsive genes reveals novel Al tolerance mechanisms in rice. *PLoS ONE* 7 (10): e48197. doi:10.1371/journal.pone.0048197.

A Acid Tolerance



B Al Tolerance

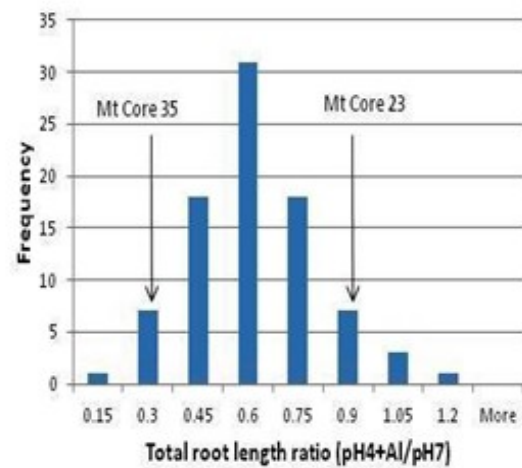


Figure 2.1: Response to acid and aluminum conditions of the *M. truncatula* core inbred lines. Mt Core 23 and Mt Core 35 used as parents to generate the RIL population.



Figure 2.2: Growth and process of inbreeding of the *M. truncatula* RIL population through multiple generations of single seed descent in a greenhouse at the Noble Foundation (Ardmore, OK).

CHAPTER 3

RESULTS AND DISCUSSION

Phenotyping for acid and aluminum responses

The root traits evaluated to assess growth response to acid pH and presence or absence of Al includes root length (RL) at pH 7, RL at pH 4, RL at pH 4+ Al 20 μ M, as well as the ratio of RL at pH 4/RL at pH 7, RL at pH 4+ Al 20 μ M/ RL at pH 7, and RL at pH 4+ Al 20 μ M/ RL at pH 4. Variables transformations were utilized to address deviations from normality for the trait variables based on the slightly, skewed phenotypic distributions of the trait histograms (Fig. 3.1 and Fig. 3.2), and used for further analysis of traits significance with the LS-Means procedure and GLIMMIX. The transformation of variable RL at pH 7, pH 4 and pH 4+ Al 20 μ M was $RL^{0.25}$ and residuals were evaluated for skewedness of the normal distribution of the transformed variable (Fig. 3.3).

From the LS-Means procedure, significant variation was observed between the mean values of $RL^{0.25}$ at pH 7, pH 4 and pH 4+ Al 20 μ M with a significant effect at $\alpha = 0.05$ due to treatment representing the different growing conditions (Table 3.1). In the GLIMMIX model, replication was used as a random effect with minimal contribution to the variation in the model (Table 3.2) and Genotype and Treatment were significant at $\alpha = 0.05$ (Table 3.3) indicating variation between the RIL genotypes as well as a response in root growth due to the different growing conditions.

The variable RL relative to RL at pH 7 (RL at pH 4/ RL at pH 7 and RL at pH4+ Al 20 μ M/ RL at pH 7) is useful to assess the relative root growth under acid and Al conditions (pH 4 and pH4+ Al 20 μ M) compared to growth at pH 7. The variable also had a skewed data distribution (Fig. 3.2) and was transformed to the Ratio pH 7^{-0.25} (RL at pH 4/ RL at pH 7)^{-0.25} and (RL at pH 4+ Al 20 μ M / RL at pH 7)^{-0.25}. Same GLIMMIX procedure was applied to this model and Genotype and Treatment were significant at $\alpha = 0.05$, while the Genotype \times Treatment interaction was not (Table 3.4). Lastly, variable Ratio pH 4 (RL at pH 7/ RL at pH 4 and RL at pH 4+ Al 20 μ M/ RL at pH 4) was also transformed to Ratio pH 4^{0.25} and from GLIMMIX procedure Genotype and Treatment were significantly different at $\alpha = 0.05$, but Genotype \times Treatment not (Table 3.5). The ratio RL at pH 4+ Al 20 μ M/ RL at pH 4 can be used as a metric to isolate the response due to the presence of Al by maintaining a consistent pH value of 4 thus, differentiating between the response due to pH vs. Al.

Genotyping

Genotyping efforts of the mapping set of the RIL population using the *M. truncatula* Golden Gate array from Illumina, yielded 190 polymorphic markers out of 1,536 SNP markers between the parental genotypes Mt Core 23 and Mt Core 35. Although these accessions were part of the *M. truncatula* nested core collections capturing the genetic variation at the sampled microsatellite loci (Han et al., 2010), the fixed SNPs on the array were selected based on their broad utility to the scientific community rather than for polymorphism in a specific set of genotypes. Also, further evaluation of genetic diversity using thousands of SNPs from the HapMap re-sequencing

initiative grouped both parental accessions in the same cluster (Yun Kang, Research Scientist at Noble Foundation, personal communication 2014), thus explaining the relatively low level of sequence diversity and thus of polymorphic markers between the parental genotypes. Moreover, of the 820 SNP markers analyzed by HRM on the parental lines, only 267 were polymorphic. Of these 102 were genotyped on RILs and used for linkage groups analysis. Only six of them were included to obtain linkage groups as the others showed skewed segregation ratios.

SNP primers that were homozygous for both parental genotypes were coded as 'a' to represent the homozygous state of the Mt Core 23 and 'b' to represent the homozygous state of the Mt Core 35, 'c' represents the heterozygote for Mt Core 23, and 'd' represents a heterozygote for the Mt Core 35 allele, and these were integrated into the linkage groups. Any SNP primers with non-specific amplification in the RIL population or with altered segregation ratios were not included in the final analysis. Overall, a total of 122 combined SNPs from the array and the AI candidate genes assayed using HRM were used for the mapping analysis.

Mapping and QTL analysis

Linkage analysis of the 122 SNP markers resulted in the generation of five linkage groups from regression mapping analysis using recombination frequencies and the Kosambi mapping function. Although we anticipated eight linkage groups to correspond to the basic chromosome number in *M. truncatula*, we were limited by the relatively low levels of SNP polymorphism between the parental genotypes and the corresponding segregation ratios in the RIL population of F_{4:5} genotypes. The successful

linkage groups (LG) generated were for LG 1, LG2, LG3, LG4 and LG5 which correspond to molecular markers physically mapped to the *M. truncatula* chromosomes 1, 2, 3, 6 and 7 respectively (Fig. 3.4). The analysis resulted in the identification of Al tolerance QTLs obtained using interval mapping (Lander and Botstein, 1989; Van Ooijen, 1992) for each of the RL traits evaluated (Fig. 3.5). The significant LOD threshold levels based on permutation test analysis for a species with eight chromosomes and 120 cM of average chromosome length ranged from 1.7 to 2.6 and 1.6 to 2.3, depending on the root length trait with a genome-wide false positive rate of 5% or 10%, respectively. Although no significant QTLs based on the LOD thresholds described above were identified using interval mapping or composite mapping, the results provided information on potential candidate QTL regions at lower LOD levels. These regions were found for RL at pH 4, RL at pH 4+ Al 20 μ M, RL at pH 4/ RL at pH 7, RL at pH 4+ Al 20 μ M,/ RL at pH 4 on LG2, LG3 and LG5.

Based on these findings, additional SNP markers were evaluated as a way to increase marker coverage on LG 2 and LG 7. A mapping study in alfalfa identified QTLs for acid and Al tolerance on LG 2 and LG 7 using a whole plant assay for the phenotypic evaluation (Khu et al, 2013). The SNP primers targeting Al tolerance in alfalfa from Khu et al. (2013) were linked to the suggestive QTLs found in this *M. truncatula* study. Despite efforts to increase marker coverage on LG 2 and LG 5 by genotyping SNPs physically mapped on *M. truncatula* chromosomes 2 and 7, the low levels of sequence variation at the sample loci between the parental genotypes hindered our ability to saturate these LGs with SNP markers.

The results from restricted composite interval mapping (rMQM) (Jansen, 1993, 1994; Jansen and Stam, 1994) did not result in the identification of any new QTL compared to the previous analysis on this study. The automatic cofactor selection (ACS) of JoinMap® 4.1 software (van Ooijen and Voorrips, 2001) was used to test the flanking markers of regions with higher LOD scores. An initial number of 19 cofactors was selected based on their position close to the maximum LOD scores per LG for each trait (Table 3.7). A fitted rMQM model that excludes the QTLs and includes the cofactors was set as a starting point for a backward elimination of the cofactors. The elimination process continued until no cofactor remains or when the change in likelihood is significant depending on the p-value for the test. The ACS provides a set of cofactors that are important for the QTL model for each trait. For the RL at pH 4, four of 19 cofactors were significant at a p-value of 0.020 (Table 3.6). One cofactor was identified for the ratio of RL at pH 4/ RL at pH 7 with a p-value of 0.020 (Table 3.6). No other cofactors representing the SNP markers were significant for the remaining four root traits evaluated. Following the ACS analysis was the implementation of a restricted composite interval mapping (rMQM) which resulted in the identification QTLs that were consistent with the interval mapping results (Fig.3.6). The rank sum test of Kruskal-Wallis was also performed assuming the non- parametric distribution of the phenotypes (Van Ooijen et al., 1993). Overall, QTLs for response to Al were identified on similar LGs although with higher LOD values (Fig. 3.7) for the root growth traits in response to low pH and aluminum compared to the previous methods.

Prediction of RIL phenotypes using SNP markers associated with acid and aluminum QTLs

The practical value of mapping studies is the identification of molecular markers that can be used as surrogates for selection of a target trait based on their ability to predict the phenotype of the lines selected. In this study, an additional 130 *M. truncatula* RILs (validation set) resulting from the same cross between Mt Core 23 \times Mt Core 35 and advanced together with the RILs used for QTL mapping were evaluated for their response to low pH and Al using the WPA (Khu et al. 2013). The RL traits evaluated for the validation set of *M. truncatula* RILs when grown under different pH and Al conditions were normally distributed (Fig. 3.8). For each of the traits evaluated (RL at pH 4, RL at pH 4+ Al 20 μ M, RL at pH 4/ RL at pH 7, RL at pH 4+ Al 20 μ M/ RL at pH 4, and RL at pH 4+ Al 20 μ M/ RL at pH 7), a selection intensity of 5% and 10% was used to identify the top and bottom 7 and 14 genotypes, respectively, for each of the traits. Overall, 14 of the 19 SNP markers flanking QTLs (used as cofactors for the rMQM mapping from previous section) were useful to predict the phenotypic response based on the genotypic data of 57 RIL lines (Table 3.6).

The mean value for the RL at pH 4 of the top 5% performers was 11.6 cm and 10.4 cm for the top 10%, while 5.2 cm and 5.5 cm for the bottom 5% and 10% performers, respectively (Table 3.7). The SNP markers evaluated on LGs 2, 3, 5 were more successful at predicting the phenotype (RL at pH 4) when a higher intensity of selection was applied (5% vs. 10%). A total of five of the seven (71.4%) individuals from the top 5% for RL at pH 4 had the allele from the tolerant parent (Mt Core 23) for SNP 467 and SNP 655 on LG 2 and SNP 1317 on LG 3, while the remaining genotypes were

heterozygous at the sampled loci. Therefore, higher selection intensity increases the likelihood of successfully identifying genotypes with better performance while reducing the probability of bringing in negative alleles for the target trait. The SNPs on LG 5 had a lower ability to predict the response and ranged from 28.6% to 57.1%. In contrast, the allele of the Mt Core 35 (sensitive parent) at SNP 1277 on LG 3 was shared among five of the total seven genotypes (71.4%) at the bottom 5% in performance. It is worth noting that SNP 475 on LG 5 had the allele from the sensitive parent (Mt Core 35) in 100% of the bottom 5% performers and 62.4% of the bottom 10% performers.

Evaluation of the RL at pH 4+ Al 20 μ M resulted in the identification of four markers with potential practical value for selection (Table 3.8). Specifically, SNP 928 on LG 5 predicted up to 71.4% of both the top 5% and the bottom 10% performers, while the prediction ability of SNP 572 and SNP 1317 both of which are located on LG 3 was 42.8%. Markers 655 and 928 from LG 5 predicted the performance of all lines with a 71.4% of efficiency (Table 3.8).

For the trait of the ratio RL at pH 4/ RL at pH 7, markers 365, 655 and 534 on LG 2 predicted 42.8% of the top 5% performers. Same markers predicted between 50% and 57.1% of the top 10% performers. The bottom 5% performers would have been correctly predicted 85.7% of the time by the markers 572 and 1317 on LG 3. The same markers predicted 57.1% of the 10% bottom performers. Also, the marker MSMAN0025 on LG 5 predicted 71.4% of the bottom 5% performer lines and 64.7% of bottom 10% lines (Table 3.9).

Evaluation of the trait RL at pH 4+ Al 20 μ M/ RL at pH 7 resulted in the identification of the markers 534 and 467 on LG 5 that predicted 57.1% of the top 5%

performer lines. Also, marker 1365 on LG 2 predicted 57.1% of the lines. For the group of the top 10 % performer lines, the markers 655 and 1209 on LG 2 predicted 57.1 % and 50% of the lines and the marker 467 on LG 5 predicted 64.3% of the lines. Markers 655 and 1209 on LG 2 predicted the bottom 5% of the RILs with an efficiency of 42.85%. The marker 1245 on LG 5 predicted the bottom 5% of the performers with an efficiency of the 42.85%. The predictive ability of marker 1245 on LG 5 at the 10% of the bottom performers increased to 57.1%, as well as, the marker 467 on LG 5 that decreased its prediction efficiency to a 50% when the number of bottom performers was extended (Table 3.10).

Analysis of the trait RL at pH 4+ Al 20 μ M/ RL at pH 4 resulted in the identification of markers 655 and 1209 on LG 2 that correctly predicted 42.8% of the top 5% performer lines and 50% of the top 10% lines. The marker 467 on LG 5 predicted 42.8% of the top 5% performers, and decreased to 35.7% when the top 10% of the lines were included. Marker 1245 on LG 5 predicted 85.7% of bottom 5% and 10% performers. Additionally, marker 467 on LG 5 predicted 71.4% and 78.6% of the bottom 5% and 10% performers (Table 3.11).

The value of the SNP markers to predict the response to Al phenotypes is directly proportional with the percentage of variability in the phenotype explained by the QTLs found. The overall pattern observed was that the SNP flanking the QTL were better able to predict the top and bottom 5% of performers compared to the top and bottom 10% of performers in the *M. truncatula* validation set of RILs. Inherently as part of QTL mapping studies with small effects as is the case with Al tolerance in *Medicago* species (Khu et al., 2013), is the underlying assumption that molecular markers from a single

QTL would not be able to predict with 100% accuracy the phenotype of the selected line . Although the Al tolerance QTL based on root growth traits identified in this study were for small effect QTLs, the number of correct predictions based on the marker alleles at the identified loci ranged from 14.3% to 100%. One should expect that markers localized within a major effect QTL would increase the frequency of identifying individuals with the desired phenotype. One should also consider the transgressive segregation patterns identified for root growth in response to pH 4 and the addition of Al to the growth medium suggesting that both parents could be contributing positive alleles for acid and Al tolerance responses. The results of mapping studies in alfalfa describing that the phenotypically inferior parent can contribute positive alleles (Narasimhamoorthy et al., 2007; Robins et al., 2007a; Robins et al., 2007b; Robins et al., 2008), is another factor worth considering. As the selection intensity shifts from 5% to 10%, the likelihood of selecting genotypes as potentially desirable while in reality these may also have negative alleles increase. Nevertheless, the results from this study show the potential value of the SNP markers as a tool for the initial selection efforts complemented by future phenotype-based confirmation of the desired target performance of the selected lines or populations.

References

- Han, Y., C.M. Motes, M.J. Monteros. 2010. Evaluation and utilization of morphological variation in a *Medicago truncatula* core collection. p. 101-105. In C. Huyghe (ed). Sustainable use of genetic diversity in forage and turf breeding. Springer Netherlands.

- Jansen R.C. 1993. Interval mapping of multiple quantitative trait loci. *Genetics* 135:205-211.
- Jansen R.C. 1994. Controlling the *type I* and *type II* errors in mapping quantitative trait loci. *Genetics* 138:871-881.
- Jansen R.C. and P. Stam. 1994. High resolution of quantitative traits into multiple loci via interval mapping. *Genetics* 136:1447-1455.
- Khu D.-M., R. Reyno, Y. Han, P.X. Zhao, J.H. Bouton, E.C. Brummer, and M.J. Monteros. 2013. Identification of aluminum tolerance quantitative trait loci in tetraploid alfalfa. *Crop Sci.* 53:148-163.
- Lander E.C. and D. Botstein. 1989. Mapping Mendelian factors underlying quantitative traits using RFLP linkage maps. *Genetics* 121: 185-199.
- Narasimhamoorthy B., J.H. Bouton, K.M. Olsen and M.K. Sledge. 2007. Quantitative trait loci and candidate gene mapping of aluminum tolerance in diploid alfalfa. *Theor. Appl. Genet* 114:901-913.10.1007/s00122-006-0488-7.
- Robins J.G., G.R. Bauman, and E.C. Brummer. 2007a. Genetic mapping forage yield, plant height, and regrowth at multiple harvests in tetraploid alfalfa (*Medicago sativa* L.). *Crop Sci.* 47:11-18.
- Robins J.G., D. Luth, I.A. Campbell, G.R. Bauman, C. L. He, D. R. Viands, J. L. Hansen, and E. C. Brummer. 2007b Genetic mapping of biomass production in tetraploid alfalfa. *Crop Sci.* 47:1-10.
- Robins J.G., D.R. Viands, and E.C. Brummer. 2008. Genetic mapping of persistence in tetraploid alfalfa. *Crop Sci.* 48:1780-1786.
- Van Ooijen J.W. 1992. Accuracy of mapping quantitative trait loci in autogamous species. *Theor. Appl. Genet.* 84:803-811.

- Van Oijen, J.W. 1993. MapQTL, a computer program for mapping quantitative trait loci. Centre for Plant Breeding and Reproduction Research. Wageningen, Netherlands.
- Van Ooijen, 2004. MapQTL[®] 5, Software for the mapping of quantitative trait loci in experimental populations. Kyazma B.V., Wageningen, Netherlands.
- Van Ooijen J.W. and R.E. Voorrips. 2001. JoinMap 3.0 software for the calculation of genetic linkage maps. Plant Research Internation, Wageningen, Netherlands.

Table 3.1: LS-Means procedure of $RL^{0.25}$ for Treatment ($\alpha = 0.05$).

Treatment	Estimate	Std Error	DF	t Value	Pr > t	
pH 7	2.4721	0.01383	3.33	178.69	<.0001	A
pH 4	1.5385	0.01387	3.362	110.94	<.0001	B
pH 4+Al	1.506	0.01387	3.365	108.57	<.0001	C

Table 3.2: Covariance parameter estimates for Replication as a random effect in the model $RL^{0.25}$.

Covariance	Estimate	Std Error
Replication	0.000381	0.000445
Residual	0.03237	0.001242

Table 3.3: *Type III* of fixed effects for $RL^{0.25}$ model ($\alpha = 0.05$).

Effect	DF	Den DF	F Value	Pr > F
Genotype	188	1359	1.63	<.0001
Treatment	2	1359	4784.9	<.0001

Table 3.4: *Type III* of fixed effects for Ratio pH 7^{-0.25} model ($\alpha = 0.05$).

Effect	DF	Den DF	F Value	Pr > F
Genotype	185	628	1.32	0.007
Treatment	1	628	6.85	0.0091
Genotype ×Treatment	184	628	0.41	1

Table 3.5: *Type III* of fixed effects for Ratio pH 4^{0.25} model ($\alpha = 0.05$).

Effect	DF	Den DF	F Value	Pr > F
Genotype	185	634	1.23	0.0343
Treatment	1	634	3104.85	<.0001
Genotype × Treatment	184	634	0.57	1

Table 3.6: Molecular markers associated with RL traits of the *M. truncatula* RIL population.

Linkage Group	SNP Id	Root trait	Cofactor	Useful to predict the genotypes of additional RIL lines
2	270	RL at pH 4, RL pH 4/ RL pH 7	No	No
2	MSCWSNP1209	RL at pH 4 +Al, RL pH 4/ RL pH 7	Yes	Yes
2	1217	RL pH 4/ RL pH 7	Yes	No
2	314	RL at pH 4	No	No
2	655	RL at pH 4	No	Yes
2	138	RL pH Al/ RL pH 7	No	No
2	1256	RL pH 4Al/ RL pH 7	No	No
2	3	RL pH 4/ RL pH 7, RL pH 4	No	No

		Al/ RL pH 7		
2	534	RL pH 4/ RL pH 7, RL pH 4Al/ RL pH 7	No	Yes
2	1365	RL pH 4/ RL pH 7, RL pH 4Al/ RL pH 7	No	Yes
3	572	RL pH 4, RL pH 4 Al, RL pH 4/ RL pH 7	No	Yes
3	1317	RL pH 4, RL pH 4 Al, RL pH 4/ RL pH 7	No	Yes
3	1277	RL at pH 4 Al	No	Yes
5	475	RL at pH 4, RL pH 4Al/ RL pH 4	Yes	Yes
5	MSMAN0045	RL at pH 4, RL pH 4/ RL pH 7, RL pH 4Al/ RL pH 4	Yes	Yes
5	MSCWSNP467	RL pH 4, RL pH 4/ RL pH 7	Yes	Yes

5	1245	RL pH 4/ RL pH 7, RL pH 4Al/ RL pH 4	No	Yes
5	928	RL at pH 4, RL pH 4/ RL pH 7	No	Yes
5	MSMAN0025	RL pH 4/ RL pH 7	No	Yes

Table 3.7: Genotype prediction of the 5% and 10% top and bottom performing RILs for the trait RL at pH 4 (RL: cm, N: negative amplification HRM reaction, U: unknown genotype class).

RL pH 4									
		LG 2			LG 3			LG 5	
Top 5%	RL pH 4	1209	655	467	1317	1277	572	MSMAN25	475
Mt23	10.0	c	a	a	a	a	a	a	a
1114	11.6	d	h	h	h	a	a	a	b
1344	11.0	d	a	a	a	h	b	h	b
1348	16.2	c	a	a	a	a	a	a	a
1351	10.0	d	a	a	a	b	a	b	b
1354	13.2	c	a	a	a	b	b	b	a
1398	9.5	d	h	h	h	a	b	a	b
1511	9.9	d	a	a	a	a	a	a	b
Mean	11.6								
% of Prediction		2/7=28.6%	5/7= 71.4%	5/7=71.4%	5/7=71.4%	4/7=57.1%	4/7=57.1%	4/7=57.1%	2/7=28.6%
Top 10%									
1170	9.5	d	b	b	h	a	a	h	b
1182	9.4	c	b	b	b	a	b	a	a
1366	9.1	d	b	b	b	a	a	a	b
1410	9.2	d	a	b	b	b	b	b	b
1424	8.9	c	b	b	b	a	b	a	a
1485	9.1	h	b	b	b	b	b	b	h
1494	9.2	d	b	b	b	b	b	b	b
Mean	10.4								
% of Prediction		4/14=28.6%	6/14=42.8%	5/14=35.7%	5/14=35.7%	8/14=57.1%	6/14=42.8%	7/14=50%	4/14=28.6%
Bottom 5%	RL pH 4	LG 2			LG 3			LG 5	
		1209	655	467	1317	1277	572	MSMAN25	475
Mt35	8.5	d	b	b	b	b	b	b	b
1216	5.0	c	a	b	h	b	h	b	b
1235	5.1	c	a	b	b	b	b	h	b
1295	4.7	N	b	N	h	a	h	N	b
1332	5.0	d	b	b	b	b	b	h	b
1408	5.6	h	h	h	h	b	h	h	b
1425	5.5	d	b	a	a	a	b	a	b
1484	5.6	c	a	h	a	b	b	h	b
Mean	5.2								
% of Prediction		2/7=28.6%	3/7=42.8%	3/7=42.8%	2/7=28.6%	5/7=71.4%	4/7=57.1%	4/7=57.1%	7/7=100%
Bottom 10%									
1174	5.7	U	a	b	b	b	b	b	b
1331	5.6	d	b	a	h	b	h	b	a
1349	5.8	c	a	h	b	a	b	b	h
1360	5.8	d	b	b	b	h	b	b	b
1457	5.7	c	a	a	b	a	b	b	a
1474	5.9	c	a	b	h	b	N	b	b
1496	5.7	c	a	a	b	b	b	b	a
Mean	5.5								
% of Prediction		4/14=28.6%	5/14=35.7%	6/14=42.8%	9/14=64.2%	9/14=64.2%	9/14=64.2%	8/14=57.1%	8/14=57.1%

Table 3.8: Genotype prediction of the 5% and 10% top and bottom performing RILs for the trait RL at pH 4+ Al 20 μ M (RL: cm).

RL pH4+Al					
	LG 2		LG 3		LG 5
Top 5%	RL pH 4+Al	655	572	1317	928
Mt23	8.1	a	a	a	a
1324	7.2	b	b	b	a
1344	7.4	b	h	h	a
1348	9.5	a	a	a	a
1351	7.7	b	b	b	a
1354	8.5	a	b	b	a
1355	7.4	b	a	a	b
1366	8.7	b	a	a	b
Mean	8.0				
% of Prediction		2/7=28.6%	3/7=42.8%	3/7=42.8%	5/7=71.4%
Top 10%					
1109	6.5	a	b	b	b
1339	6.8	a	b	b	h
1374	6.6	a	a	a	a
1378	6.6	h	a	a	b
1382	7.1	b	h	h	b
1410	7.1	b	b	b	a
1492	6.6	a	a	a	a
Mean	7.4				
% of Prediction		6/14=42.8%	6/14=42.8%	6/14=42.8%	6/14=42.8%
		LG 2	LG 3		LG 5
Bottom 5%	RL pH 4+Al	655	572	1317	928
Mt35	3.6	b	b	b	b
1115	3.7	b	a	a	b
1175	3.3	h	h	h	b
1297	2.6	b	b	b	b
1421	3.7	a	a	h	h
1456	2.8	b	a	a	a
1462	3.5	b	b	b	h
1483	3.8	b	a	a	b
Mean	3.3				
% of Prediction		5/7=71.4%	2/7=28.6%	2/7=28.6%	4/7=57.1%
Bottom 10%	RL pH 4+Al				
1216	3.9	a	h	h	b
1342	3.9	a	a	a	b
1395	3.9	b	a	h	b
1398	4.0	b	a	a	b
1438	3.8	a	b	b	b
1484	3.8	a	a	b	h
1510	4.0	a	b	b	b
Mean	3.6				
% of Prediction		7/14=50%	5/14=35.7%	5/14=35.7%	10/14=71.4%

Table 3.9: Genotype prediction of the 5% and 10% top and bottom performing RILs for the trait RL at pH 4/ RL at pH 7 (N: negative HRM amplification reaction, U: unknown genotype class).

RL pH4/RL pH7												
		LG 2				LG 3		LG 5				
Top 5%	RL Ratio	1209	1365	655	534	572	1317	467	928	1245	MSMAN25	MSMAN45
Mt23	0.4	c	a	a	a	a	a	a	a	a	a	a
1220	0.5	d	a	b	a	h	h	a	h	h	h	a
1295	0.7	N	a	b	a	h	h	N	b	b	N	N
1410	1.3	d	a	b	a	b	b	a	a	a	a	b
1438	0.6	d	h	a	h	b	b	b	b	b	b	b
1474	0.8	c	h	a	h	N	h	b	b	b	b	b
1492	1.2	c	b	a	b	a	a	a	a	a	a	a
1504	0.7	d	b	b	b	b	b	b	b	b	h	b
Mean	0.8											
% of Prediction		2/7=28.6%	3/7=42.8%	3/7=42.8%	3/7=42.8%	1/7=14.3%	1/7=14.3%	3/7=42.8%	2/7=28.6%	2/7=28.6%	2/7=28.6%	2/7=28.6%
Top 10%	RL Ratio											
1511	0.3	d	h	b	h	a	a	a	a	a	a	a
1485	0.3	h	h	h	h	b	b	b	b	b	b	b
1421	0.3	c	a	a	a	a	a	b	b	b	b	b
1354	0.4	c	a	a	a	b	b	a	a	a	a	a
1424	0.4	c	a	a	a	a	a	b	b	b	b	b
1114	0.4	d	a	b	a	a	a	h	h	h	h	h
1490	0.4	c	a	a	a	b	b	a	a	a	a	a
Mean	0.6											
% of Prediction		6/14=42.8%	8/14=57.1%	7/14=50%	8/14=57.1%	5/14=35.7%	5/14=35.7%	6/14=42.8%	5/14=35.7%	5/14=35.7%	5/14=35.7%	5/14=35.7%
		LG 2				LG 3		LG 5				
Bottom 5%	RL Ratio	1209	1365	655	534	572	1317	467	928	1245	MSMAN25	MSMAN45
Mt35	0.3	d	b	b	b	b	b	b	b	b	b	b
1349	0.2	c	a	a	a	b	b	h	b	b	b	h
1360	0.1	d	a	b	a	b	b	b	b	b	b	b
1425	0.1	d	b	b	b	b	b	a	a	a	a	b
1457	0.1	c	b	a	b	b	b	a	b	b	b	a
1465	0.1	h	b	h	b	h	a	b	b	b	b	b
1484	0.1	c	h	a	h	b	b	h	h	h	h	h
1496	0.1	c	a	a	a	b	b	a	a	a	b	a
Mean	0.1											
% of Prediction		3/7=42.8%	3/7=42.8%	2/7=28.6%	3/7=42.8%	6/7=85.7%	6/7=85.7%	2/7=28.6%	4/7=57.1%	4/7=57.1%	5/7=71.4%	3/7=42.8%
Bottom 10%	RL Ratio											
1174	0.2	U	a	a	a	b	b	b	b	b	b	b
1216	0.2	c	b	a	b	h	h	b	b	b	b	b
1235	0.2	c	a	a	a	b	b	b	b	b	h	b
1272	0.2	h	h	h	h	a	a	a	a	a	a	a
1331	0.2	d	b	b	b	h	h	a	b	b	b	a
1356	0.2	c	b	a	b	b	b	h	h	h	a	h
1408	0.2	h	h	h	h	h	h	h	h	h	h	h
Mean	0.2											
% of Prediction		3/14=21.4%	6/14=42.8%	3/14=21.4%	6/14=42.8%	9/14=64.3%	9/14=64.3%	5/14=35.7%	7/14=50%	8/14=57.1%	8/14=57.1%	6/14=42.8%

Table 3.10: Genotype prediction of the 5% and 10% top and bottom performing RILs for the trait RL at pH 4+ Al 20 μ M/ RL at pH 7 (N: negative HRM amplification reaction; U: unknown genotype class)).

RL pH4Al/RL pH7							
		LG 2				LG5	
Top 5%	RL Ratio	655	1209	1365	534	467	1245
Mt23	0.2033	a	c	a	a	a	a
1220	0.388039	b	d	a	a	a	h
1490	0.3966745	a	c	a	a	a	a
1504	0.4505504	b	d	b	b	b	b
1295	0.8992095	b	U	a	a	U	b
1410	0.9592792	b	d	a	a	a	a
1492	1.3441642	a	c	b	b	a	a
1474	1.757185	a	c	h	h	b	b
Mean	0.8850145	3/7=42.85%	3/7=42.85%	4/7=57.1%	4/7=57.1%	4/7=57.1%	3/7=42.85%
% of Prediction							
Top 10%	RL Ratio						
1355	0.2338526	b	d	b	b	a	b
1354	0.2340993	a	c	a	a	a	a
1339	0.2342152	a	c	b	b	a	h
1351	0.245808	b	d	b	b	a	a
1348	0.25324	a	c	b	b	a	a
1424	0.26658	a	c	a	a	b	b
1438	0.385712	a	d	h	h	b	b
1220	0.388039	b	d	a	a	a	h
1490	0.3966745	a	c	a	a	a	a
1504	0.4505504	b	d	b	b	b	b
1295	0.8992095	b	U	a	a	U	b
1410	0.9592792	b	d	a	a	a	a
1492	1.3441642	a	c	b	b	a	a
1474	1.757185	a	c	h	h	b	b
Mean	0.5749006	8/14=57.1%	7/14=50%	6/14=42.85%	6/14=42.8%	9/14=64.3%	6/14=42.8%
% of Prediction							
		LG 2				LG 5	
Bottom 5%	RL Ratio	1209	655	1365	534	467	1245
Mt35	0.145	d	b	b	b	b	b
1297	0.0681275	d	b	b	b	b	b
1175	0.0969025	h	h	N	a	b	b
1484	0.0977599	c	a	h	h	h	h
1462	0.0981868	d	b	a	a	b	h
1182	0.0986315	c	a	a	a	b	h
1395	0.104688	d	b	b	b	b	b
1283	0.1123742	c	a	a	a	a	a
Mean	0.0940494						
% of Prediction		3/7=42.85%	3/7=42.85%	2/7=28.6%	2/7=28.6%	5/7=71.4%	3/7=42.85%
Bottom 10%	RL Ratio						
1297	0.0681275	d	b	b	b	b	b
1175	0.0969025	h	h	N	a	b	b
1484	0.0977599	c	a	h	h	h	h
1462	0.0981868	d	b	a	a	b	h
1182	0.0986315	c	a	a	a	b	h
1395	0.104688	d	b	b	b	b	b
1283	0.1123742	c	a	a	a	a	a
1356	0.1130166	c	a	b	b	h	h
1115	0.1137782	d	b	b	b	b	b
1398	0.11446	d	b	a	a	h	b
1349	0.1148322	c	a	a	a	h	b
1179	0.1166689	d	b	b	b	h	b
1465	0.11838	h	h	b	b	b	b
1272	0.1187561	h	h	h	h	a	a
Mean	0.106183						
% of Prediction		6/14=42.8%	6/14=42.8%	6/14=42.8%	6/14=42.8%	7/14=50%	8/14=57.1%

Table 3.11: Genotype prediction of the 5% and 10% top and bottom performing RILs for the trait RL at pH 4+ Al 20 µM/ RL at pH 4 (N: negative HRM amplification reaction) .

RL pH4Al/ RL pH4		LG 2			LG 5			
Top 5%	RL Ratio	655	1209	1365	467	475	1245	MSMAN45
Mt23	0.7	a	c	a	a	a	a	a
1339	1.0	a	c	b	a	a	h	a
1365	1.0	a	c	h	b	b	b	b
1324	1.1	b	d	a	a	a	a	a
1474	1.1	a	c	h	b	b	b	b
1366	1.1	b	d	b	b	b	b	b
1425	1.4	b	d	b	a	b	a	b
1332	1.4	b	d	b	b	b	N	b
Mean	1.2							
% of Prediction		3/7=42.8%	3/7=42.8%	1/7=14.3%	3/7=42.8%	2/7=28.6%	2/7=28.6%	2/7=28.6%
Top 10%	RL Ratio	LG 2			LG 5			
1154	0.9	a	c	h	b	a	b	a
1360	0.9	b	d	a	b	b	b	b
1378	0.9	h	h	a	b	b	b	b
1235	1.0	a	c	a	b	b	b	b
1374	1.0	a	c	b	a	a	a	a
1408	1.0	h	h	h	h	h	h	h
1348	1.0	a	c	b	a	a	a	a
1339	1.0	a	c	b	a	a	h	a
1365	1.0	a	c	h	b	b	b	b
1324	1.1	b	d	a	a	a	a	a
1474	1.1	a	c	h	b	b	b	b
1366	1.1	b	d	b	b	b	b	b
1425	1.4	b	d	b	a	b	a	b
1332	1.4	b	d	b	b	b	N	b
Mean	1.1							
% of Prediction		7/14=50%	7/14=50%	4/14=28.6%	5/14=35.7%	5/14=35.7%	4/14=28.6%	5/14=35.7%
Bottom 5%	RL Ratio	655	1209	1365	467	475	1245	MSMAN45
Mt35	0.4	b	d	b	b	b	b	b
1175	0.5	h	h	N	b	b	b	b
1182	0.5	a	c	a	b	b	h	b
1297	0.4	b	d	b	b	b	b	b
1398	0.4	b	d	a	h	h	b	h
1421	0.5	a	c	a	b	b	b	b
1457	0.0	a	c	b	a	a	b	a
1510	0.4	a	c	b	b	h	b	h
Mean	0.4							
% of Prediction		2/7=28.6%	2/7=28.6%	3/7=42.8%	5/7=71.4%	4/7=57.1%	6/7=85.7%	4/7=57.1%
Bottom 10%	RL Ratio	LG 2			LG 5			
1114	0.5	b	d	a	h	h	h	h
1115	0.5	b	d	b	b	b	b	b
1175	0.5	h	h	N	b	b	b	b
1182	0.5	a	c	a	b	b	h	b
1297	0.4	b	d	b	b	b	b	b
1395	0.5	b	d	b	b	b	b	b
1398	0.4	b	d	a	h	h	b	h
1421	0.5	a	c	a	b	b	b	b
1438	0.6	a	d	h	b	b	b	b
1457	0.0	a	c	b	a	a	b	a
1462	0.5	b	d	a	b	a	b	b
1483	0.6	b	d	h	b	b	b	b
1494	0.6	b	d	a	b	b	b	b
1510	0.4	a	c	b	b	h	b	h
Mean	0.5							
% of Prediction		8/14=57.1%	9/14=64.3%	5/14=35.7%	11/14=78.6%	9/14=64.3%	12/14=85.7%	10/14=71.4%

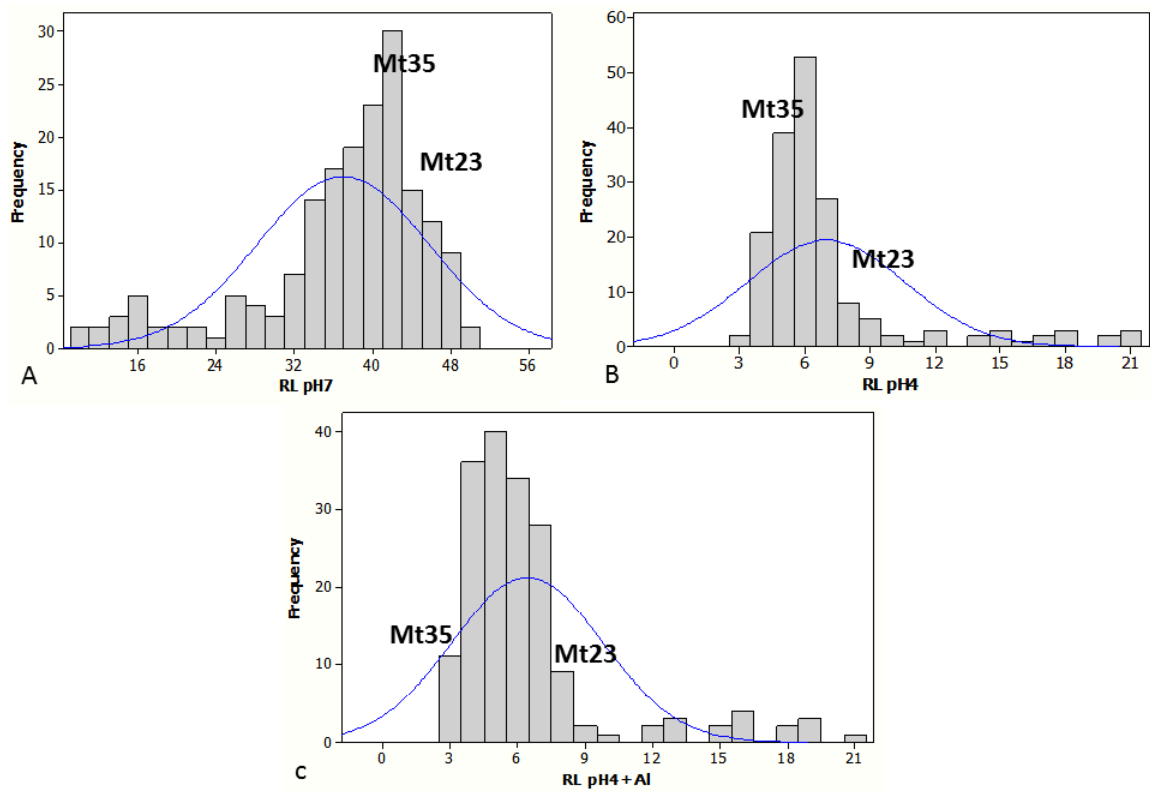


Figure 3.1: Phenotype distributions for the RIL mapping population A) RL at pH 7, B) RL at pH 4, C) RL at pH 4+ Al 20 μ M.

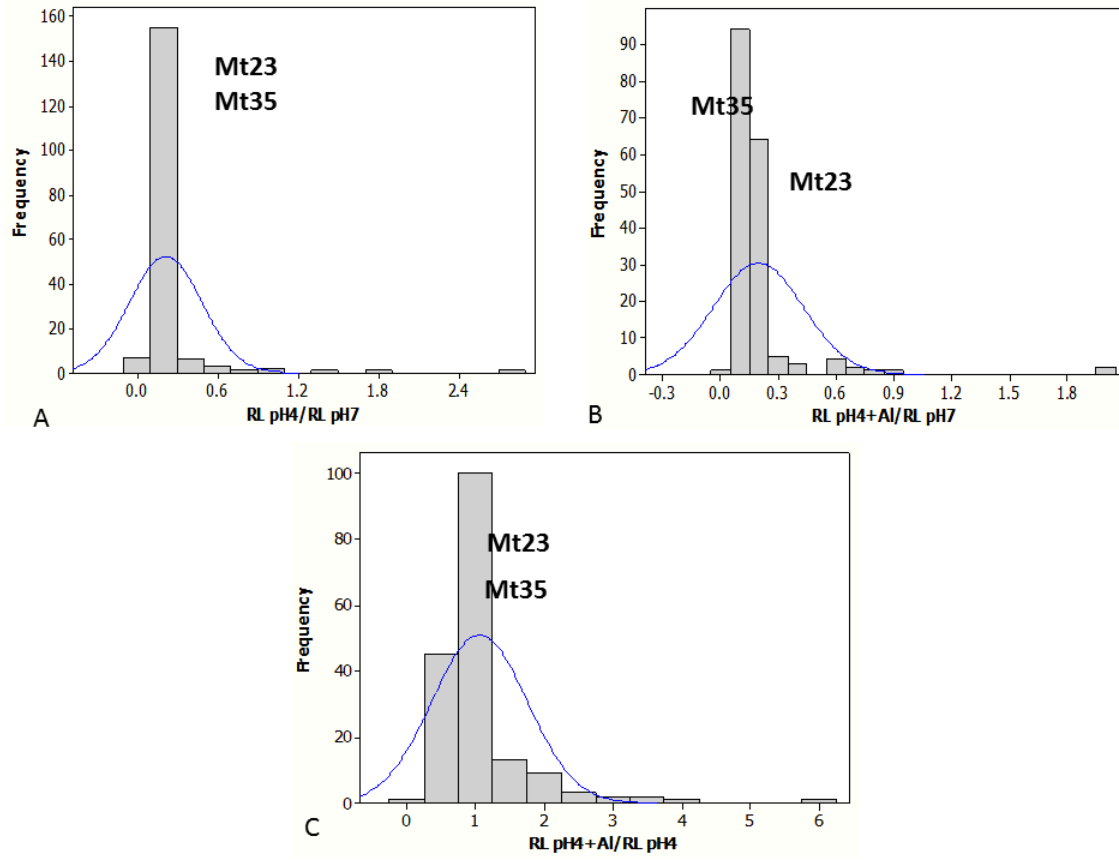


Figure 3.2: Phenotype distributions for the RIL mapping population A) RL at pH 4/ RL at pH7, B) RL at pH 4+ Al 20 μ M/ RL at pH 7, C) RL at pH 4+ Al 20 μ M/ RL at pH 4.

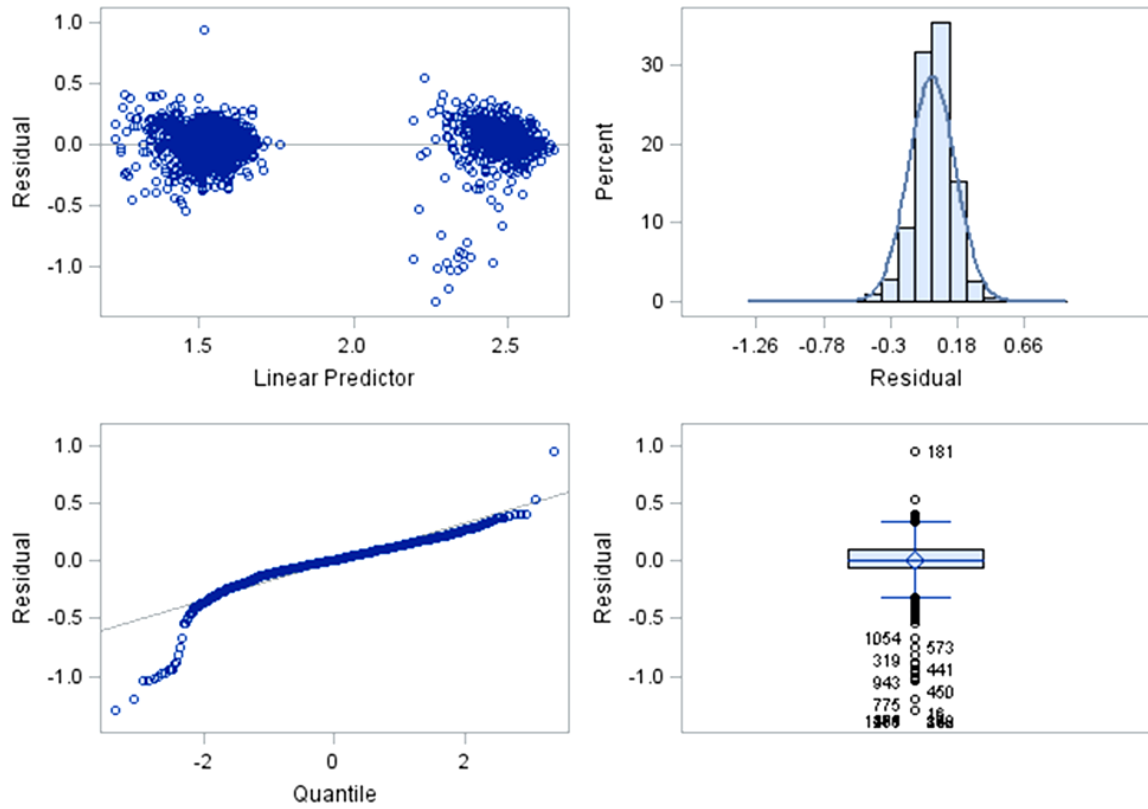


Figure 3.3: Conditional residuals for variables of the $RL^{-0.25}$ phenotypes analyzed with the GLIMMIX procedure.

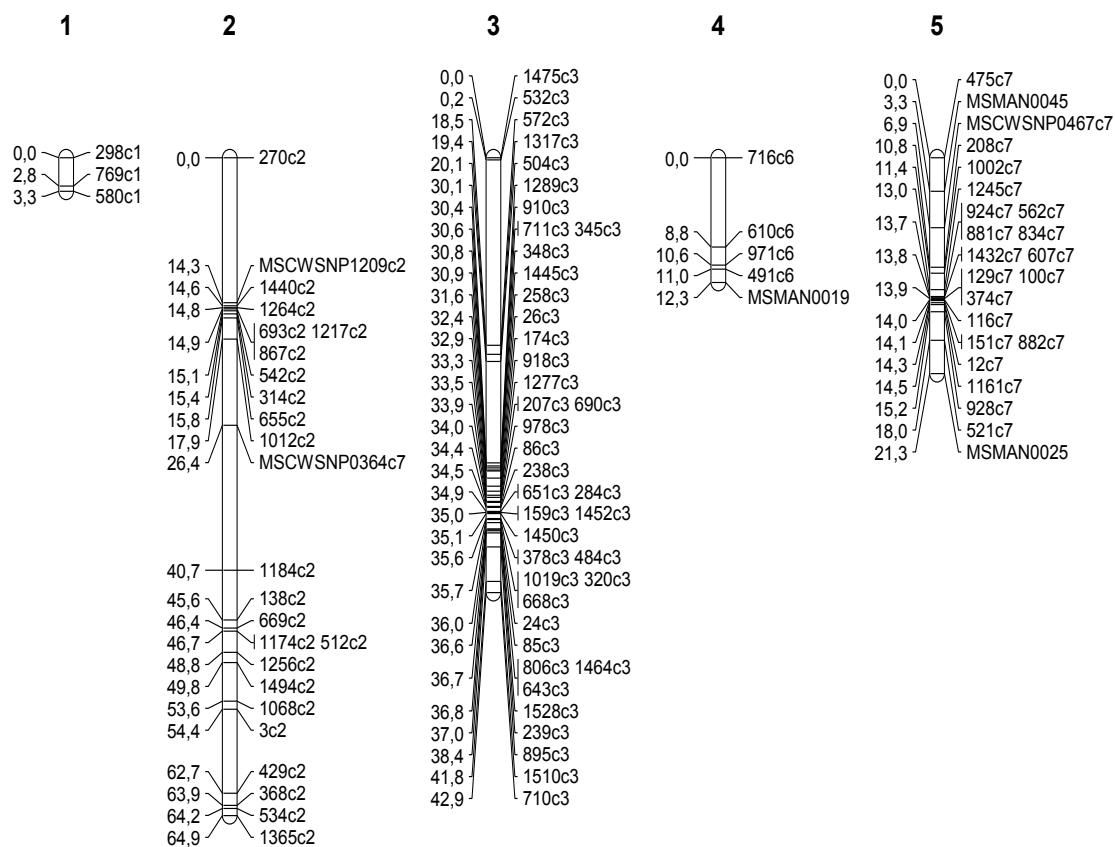


Figure 3.4: Linkage groups obtained and used for mapping Al tolerance genomic regions in the *M. truncatula* RIL population.

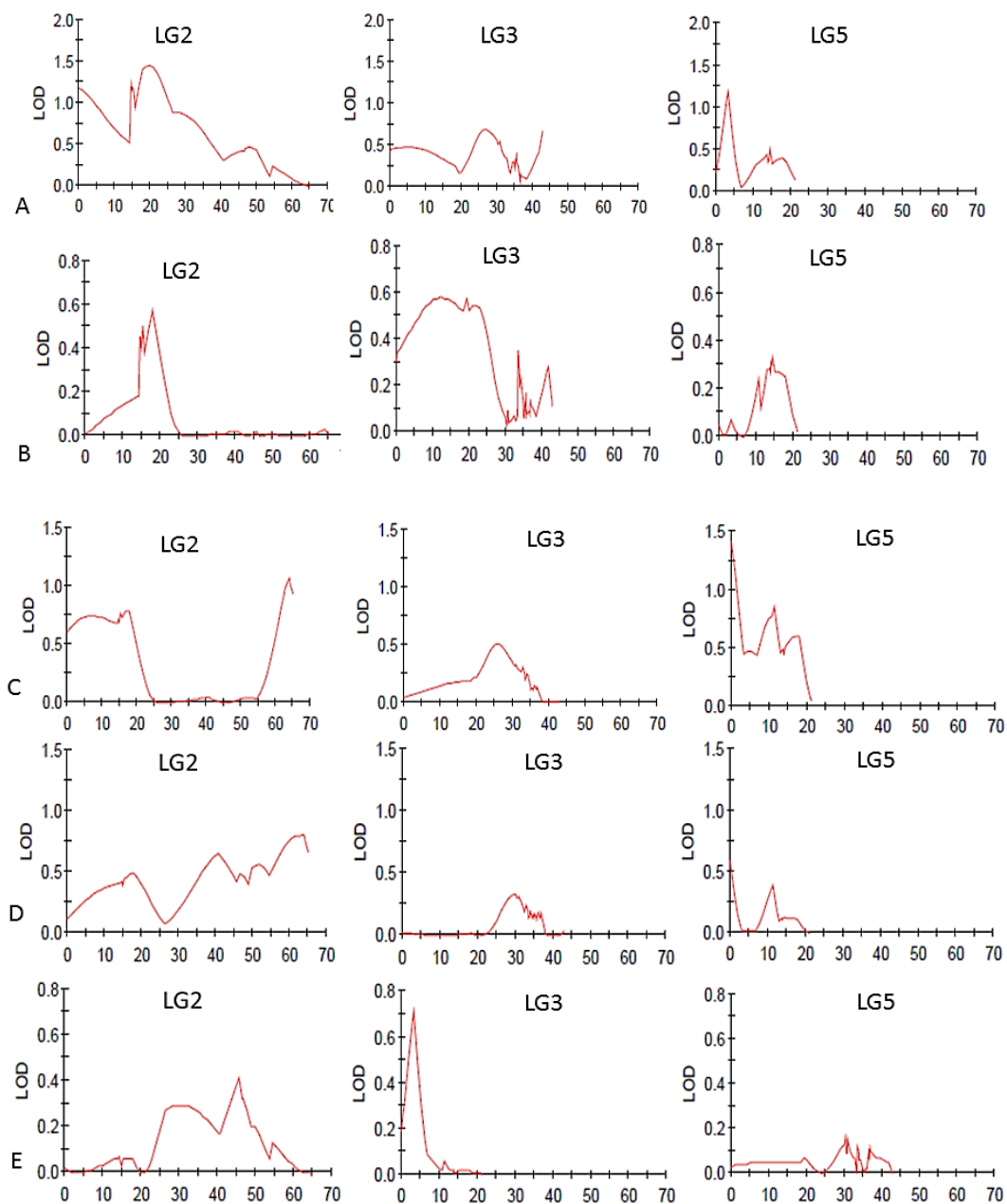


Figure 3.5: QTLs detected in the *M. truncatula* RIL population by interval mapping for the different root length (RL) traits A) RL at pH 4, B) RL at pH 4+ Al 20 μ M, C) RL at pH4/ RL at pH 7, D) RL at pH 4+ Al 20 μ M/ RL at pH7, E) RL at pH 4+ Al 20 μ M/ RL at pH4. (The X axis represents the cM position and the Y axis represents the LOD values).

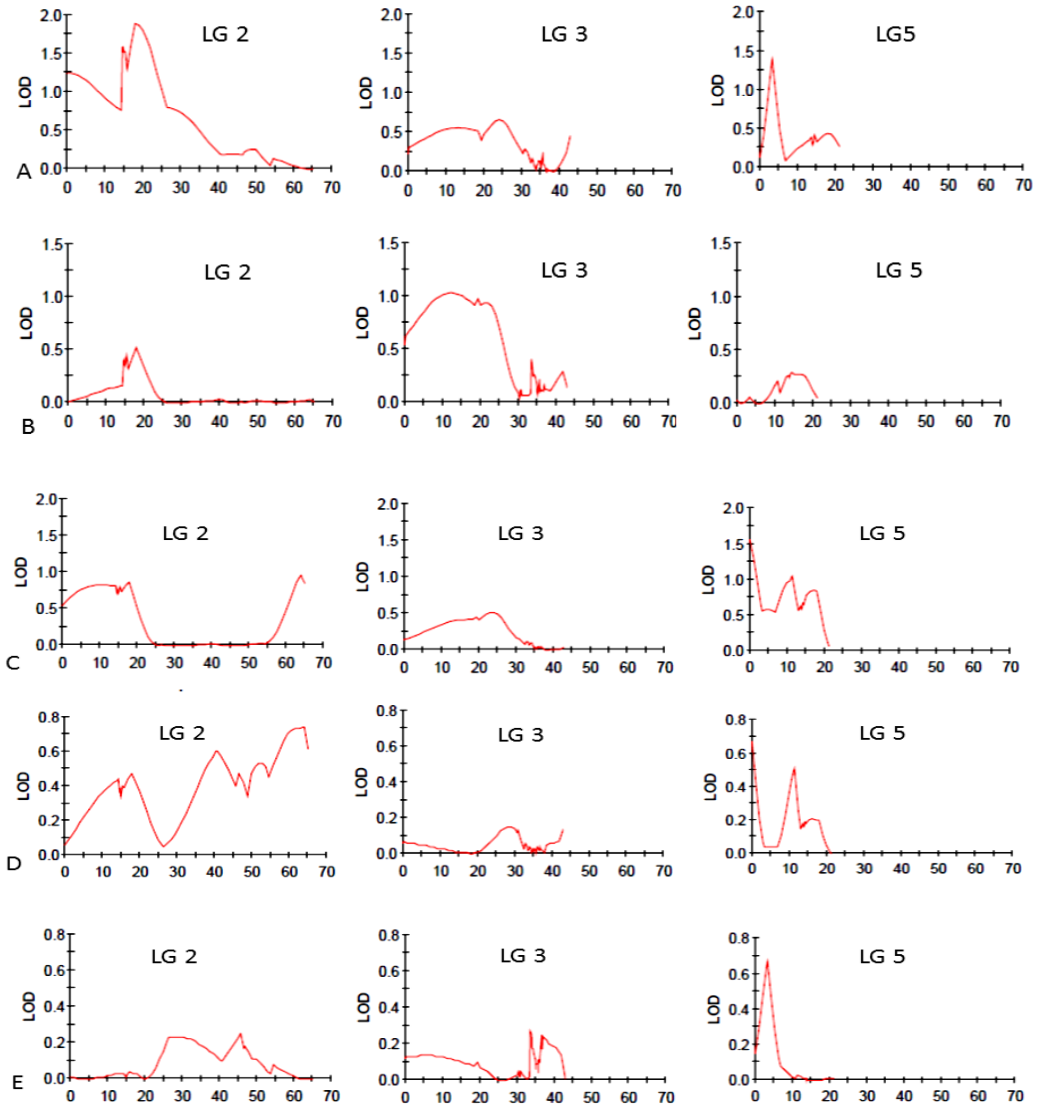


Figure 3.6: QTLs detected in the *M. truncatula* RIL population by rMQM for the different root length (RL) traits A) RL at pH 4, B) RL at pH 4+ Al 20 μ M, C) RL at pH 4/ RL at pH 7, D) RL at pH 4+ Al 20 μ M/ RL at pH7, E) RL at pH 4+ Al 20 μ M/ RL at pH4.(The X axis represents the cM position and the Y axis represents the LOD values).

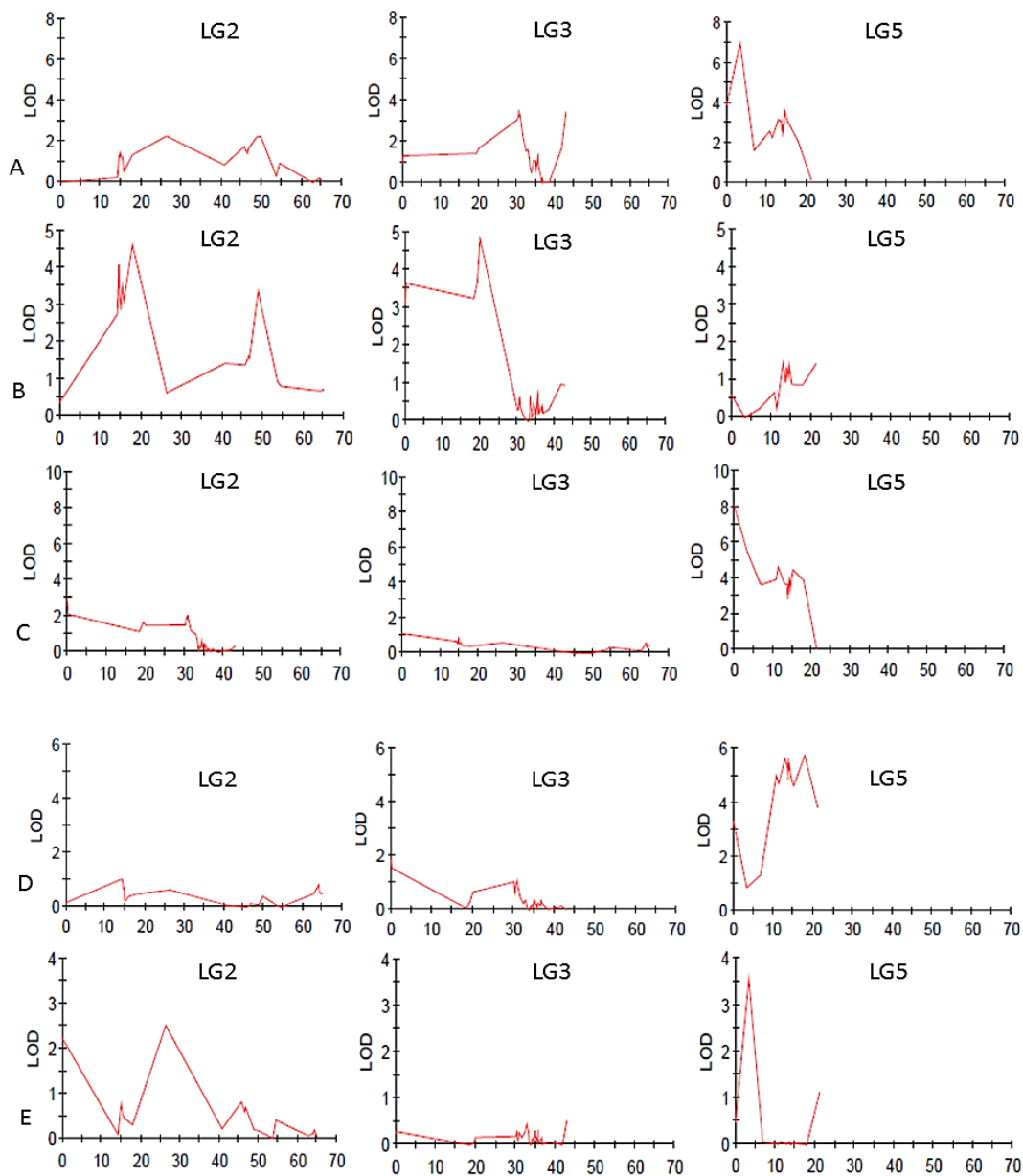


Figure 3.7: QTLs detected in the *M. truncatula* RIL population by Kruskal-Wallis non-parametric mapping for the different root length (RL) traits A) RL at pH 4, B) RL at pH 4+ Al 20 μ M, C) RL at pH 4/ RL at pH 7, D) RL at pH 4+ Al 20 μ M/ RL at pH7, E) RL at pH 4+ Al 20 μ M/ RL at pH4. (The X axis represents the cM position and the Y axis represents the LOD values).

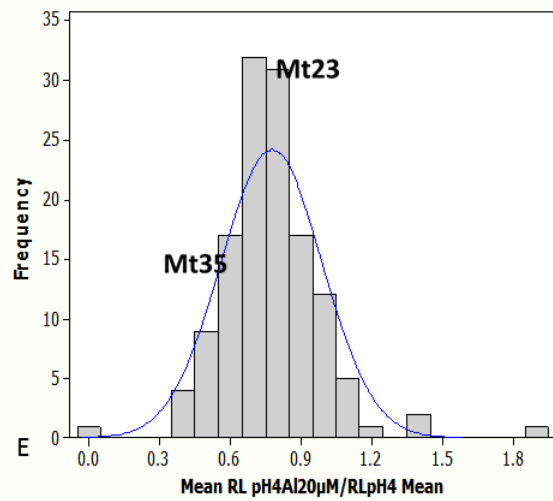
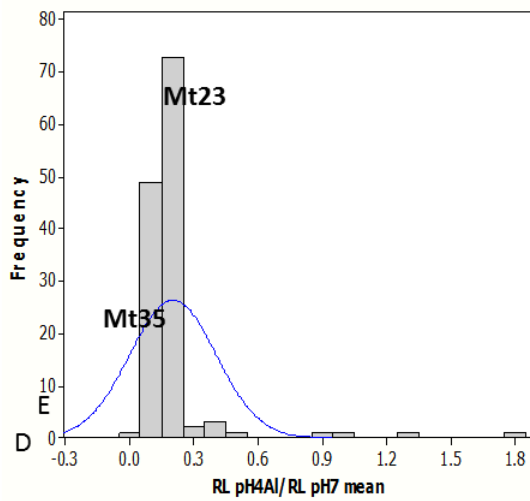
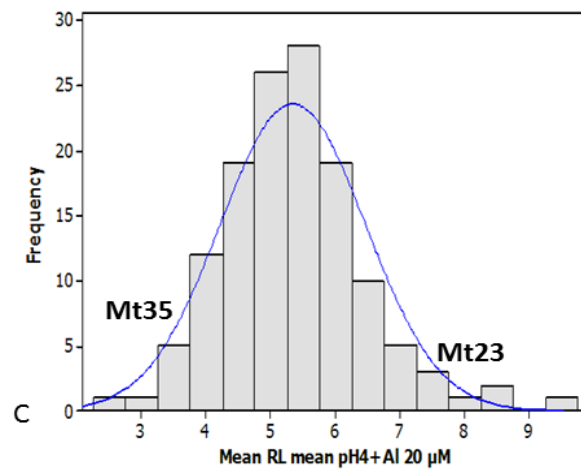
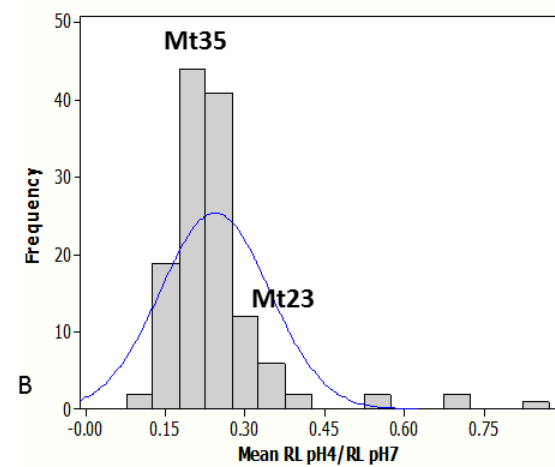
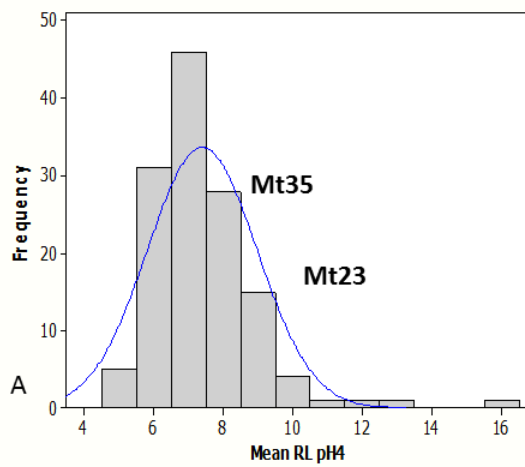


Figure 3.8: Mean phenotype distributions for the RILs used to predict phenotypes based on markers associated to QTLs for the root length (RL) traits A) RL at pH 4, B) RL at pH 4/ RL at pH 7, C) RL at pH 4+ Al 20 μ M and D) RL at pH 4+Al 20/ RL at pH 7, E) RL at pH 4+Al 20 μ M/ RL at pH 4.

CHAPTER 4

OTHER STRATEGIES TO UNDERSTAND ACID AND ALUMINUM TOLERANCE:

GENE EXPRESSION OF STRESS, ACID AND ALUMINUM TOLERANCE

CANDIDATE GENES

Introduction

Another strategy to understand the mechanisms of aluminum tolerance and resistance in plants is to evaluate the gene expression patterns of genes that are involved in different aspects of the aluminum tolerance and resistance. The genes are involved with plants general stress responses or some others are specific for Al stress responses. Mentioned genes had been found on previous studies to be differentially expressed in response to the plant growth on media with and without Al. Mentioned genes include organic acid synthesis enzymes and transporters (specifically activated under Al treatment), peroxidases, thioredoxins, dehydrin and metal ion binding genes (associated with general stress responses) (Barone et al., 2008; Chandran et al., 2008a; Chandran et al., 2008b; Iuchi et al., 2007; Khu et al., 2013). All these genes were tested in the parents of the RIL population for a differential gene expression under acid and Al treatments.

Materials and methods

The *M. truncatula* genotypes Mt Core 23 and Mt Core 35 were grown using a WPA as previously described (Chapter 2). The experimental design included six replications per genotype grown for 14 days in each of the following conditions: pH 7,

pH 4, and pH 4+ Al 20 μ M. Roots and leaves were harvested and flash frozen in liquid nitrogen and maintained at -80°C until sample processing. Total RNA was extracted from leaf and root tissue separately which was pooled from three replications per parental line, following the Maxwell® 16 LEV Plant RNA kit with the Maxwell® 16 Research Instrument (Promega, Madison, WI). Quantification and quality of the extracted RNA were evaluated using a 2100 BioAnalyzer (Agilent Technologies, Waldbronn, Germany), which is a gel base system that shows two peaks each of which corresponds to 18S and 28S present in the RNA, using RNA 6000 Nano Chips (Agilent Technologies, Waldbronn, Germany). Isolated RNA was subjected to Turbo DNA-free™ kit (Ambion, Carlsbad, CA, USA) treatment to remove genomic DNA. The quality of RNA without any DNA was confirmed via qPCR using an ABI PRISM® 7900 HT Sequence Detection System (Applied Biosystems, Foster City, CA, USA) with intron primers targeting the *Ubiquitin* gene as a control. A total of 50 ng of RNA (from all tissue and treatment samples) was reversed transcribed using the SuperScript III Reverse Transcriptase (Invitrogen GmbH, Karlsruhe, Germany), the oligo-dT₁₂₋₁₈ (Invitrogen, Carlsbad, CA, USA) to start the reaction and the RNase OUT™ Recombinant Ribonuclease Inhibitor (Invitrogen, Carlsbad, CA, USA) following the manufacturer's protocols. To check the cDNA efficiency, qPCR was performed to amplify segments on the 5' and 3' regions of the *Ubiquitin* cDNA. The ΔC_T (Ct_{3'} - Ct_{5'}) was less or equal to two and therefore cDNA samples were considered of a good quality to use in qRT-PCR analysis.

The primer design for the qRT-PCR experiments was based on the acid and Al tolerance candidate genes and other genes previously reported to be differentially

expressed in response to Al and acid treatments (Barone et al., 2008; Chandran et al., 2008a; Chandran et al., 2008b; Iuchi et al., 2007; Khu et al., 2013). Coding sequences of candidate genes from chromosomes 2 and 7 (location of Al tolerance QTLs in the *M. truncatula* RILs), as well as other relevant chromosomes were targeted in this experiment. The candidate genes evaluated included organic acid transporters and enzymes, peroxidases, metal ion binding proteins, thioredoxins and other Al and acid stress related genes (Table 4.1). Sequences were obtained from the International *Medicago* Genome Annotated Group (IMGAG) V3.5 V3 and the *M. truncatula* Gene Index (MTGI) V10.0. The *Medicago truncatula* Gene Expression Atlas (<http://mtgea.noble.org/v3/>) served to evaluate the expression level of some of the genes in specific target tissues, with particular interest in those expressed in the roots given that the roots are the main site in which acid and Al toxicity occurs (Kochian et al., 2005). The software Primer Express (v. 2.0, Applied Biosystems, Foster City, CA, USA) was used to design primers based on the following criteria: melting temperatures ranging between 58°C to 61°C, amplicon length of 60-120 base pairs and limited self-complementarity and poly-X (Supplementary Table 4.1) (Rozen and Skaletsky, 2000). qPCR reactions were performed in the ABI PRISM® 7900HT (Applied Biosystems, Foster, CA, USA) thermocycler using the SYBR® Green fluorescence dye to quantify cDNA. Reactions were performed by triplicate in a final volume of 10 µl with 2 µl of primer pair mix at 1 µM, 5 µl of KiCqStart® SYBR® Green Ready Mix™ (Sigma-Aldrich, Saint Louis, MO, USA), 1 µl of water, and 2 µl of 1:5 dilution of the cDNA. The PCR protocol included a hold at 50°C for 2 min, 95°C for 10 min, followed by 40 cycles

of 95°C for 15 sec and 60°C for 1 min, with melting curves obtained after 40 cycles of heating and cooling down (Kakar et al., 2008).

Data analysis was performed using the SDS 2.2.1 software (Applied Biosystems, Foster City, CA, USA). PCR efficiencies were checked for their proximity to a value of two using the LinReg software as described by Ramakers et al. 2003. The Delta-Delta method for comparing relative expression results between treatments was performed, following the formula $2^{-\Delta\Delta C}$ (Livak and Schmittgen, 2001; Pfaffl, 2001). Mean C_T values of each sample were normalized against the geometric mean of the three control genes UBC9 (*Ubiquitin*), *Helicase* and *actin 2* (Vandesompele et al., 2002; Kakar et al., 2008) obtaining the ΔC_T . The geometric mean was used as a way to normalize the range of C_T values of the three housekeeping genes by giving each housekeeping genes the same weight when averaged.

Results and discussion

Differential gene expression in response to pH and aluminum was identified in the *M. truncatula* parental genotypes used to generate the QTL mapping population. The dehydrine gene (Medtr7g086340) coded a protein associated with responses to stresses including cold acclimation and prevention of desiccation (Yang et al., 2012). This protein was previously found to be highly expressed in *M. truncatula* grown under Al stress (Chandran et al., 2008a) and was also related to genomic regions associated with Al tolerance in alfalfa (Khu et al., 2013). This gene is expressed at higher levels in root tissues of Mt Core 35 compared to Mt Core 23 at pH 4 and pH 4 +Al vs. pH 7 (Fig. 4.1A), indicating that this gene is responsive to Al stress. In addition to the changes in

expression in response to Al, the change in expression was also observed under acid conditions. The fold change in relative gene expression for both parental genotypes when comparing pH 4 vs. pH 4 +Al treatments was higher for Mt Core 23 than for Mt Core 35 (Fig. 4.1B). This observation could indicate that the dehydrine is expressed at higher levels to protect tissues from the Mt Core 23 from cellular damage caused by Al. In leaf tissue, Mt Core 23 had a higher fold change in relative gene expression than Mt Core 35 when comparing acid and Al conditions to pH 7 (Fig. 4.2A). The parental genotype Mt Core 35 had a higher fold change in expression at pH 4 +Al relative to pH 4 than the Mt Core 23 (Fig. 4.2B).

The citrate synthase is an enzyme that is involved in the TCA cycle and plays a role in the organic acid citrate production and release as part of Al tolerance mechanisms in a variety of plants (Ma et al., 2001; Kochian et al., 2005). In root tissues, the fold change in relative gene expression of the citrate synthase (Medtr5g091930) gene is higher in Mt Core 35 than Mt Core 23 when comparing the pH 4 and pH 4+Al treatments to pH 7. There is a clear difference between both genotypes in the fold change in expression when comparing pH 4 +Al to pH 7, further supporting the role of the citrate synthase in Al tolerance mechanisms (Fig. 4.3A). Mt Core 35 showed a higher fold change when the gene expression of pH 4 +Al treatment was compared to pH 4 (Fig. 4.3B). Previous work supports the idea that the accumulation of enzymes and organic acids in plants exposed to Al stress is not immediate (Anoop et al., 2003; Chandran et al., 2008a). In this experiment, the relative gene expression was evaluated after 14 days of growth only and no clear differences in gene expression were identified at this single time-point. Although the exudation of organic acids is an important mechanisms of Al tolerance, it is not the

only mechanisms of tolerance. A study comparing Al tolerant and sensitive wheat lines showed that all lines exhibited a significant Al activated citrate exudation and one of the sensitive lines had the largest citrate exudation (Piñeros et al., 2005). Another gene sequence of the citrate synthase (Medtr3g048920) showed a similar pattern as previously described in wheat when comparing gene expression at pH 4 and pH 4 +Al treatments with pH 7 (Fig. 4.4A). In addition, the fold change in relative expression at pH4 +Al when compared to pH 4 was also higher in the root tissues of Mt Core 35 vs the Mt Core 23 (Fig. 4.4B). However, the tendency was the opposite in leaf tissue for which the gene expression was higher for Mt Core 23 (data no shown). The tissue-specific differential gene expression of a citrate synthase gene was also reported for potatoes (Landschütze et al., 2001).

The malate dehydrogenase is another enzyme involved in the TCA cycle and has been found to play a role in the tolerance to Al toxicity in plants (Kochian et al., 2005). The fold change in the malate dehydrogenase gene (Medtr2g045010) gene expression at pH 4 and pH 4 +Al relative to pH 7 was higher in root tissues of the Mt Core 35 compared to the Mt Core 23 (Fig. 4.5A). The fold change in the relative gene expression between pH 4 + Al and pH 4 treatments follows the same pattern previously described for the Mt Core 35 (Fig. 4.5B).

The citrate transporter is an electrochemical potential- driven transporter activated by Al and it belongs to the multidrug and toxic compound extrusion (*MATE*) family (Magalhaes, 2010). There was a higher fold change in the citrate transporter (Medtr8g036660) relative gene expression in root tissues between pH 4 +Al and pH 7 for Mt Core 35 than for Mt Core 23 (Fig. 4.6A). However, the fold change in relative gene

expression between pH 4 +Al and pH 4 is higher for Mt Core 23 than Mt Core 35, suggesting that citrate production induced as a response to Al could be transported to or from the roots in Mt Core 23 (Fig. 4.6B). A second gene sequence of the citrate transporter (Medtr7g070210) was also evaluated and the patterns of changes in relative gene expression between pH 4 +Al and pH 4 treatments were consistent with the first citrate transporter gene (Fig. 4.6C).

The malate transporter is an electrochemical potential-driven transporter activated by Al and belongs to the aromatic acid exporter (*ArAE*) family (Ma, 2000; Ma et al., 2001; Ryan and Delhaize, 2001, Sasaki et al., 2004). The fold changes in relative gene expression of the malate transporter (Medtr8g104120) was higher in roots of the Mt Core 35 compared to the Mt Core 23 considering expression at pH 4 vs. pH 7 and pH 4 +Al vs. pH 7 treatments (Fig. 4.7A). However, the change in relative gene expression of the transporter in root tissue of Mt Core 23 was higher when comparing pH 4 +Al and pH 4 (Fig. 4.7B).

A metal ion binding protein related with heavy metal transport and detoxification found to be up-regulated in response to Al treatment in both sensitive and tolerant plants from previous work in *M. truncatula* (Chandran et al., 2008a), was evaluated for expression levels between Mt Core 23 and Mt Core 35. The fold change in relative gene expression of the Medtr7g100450 was higher in root tissues of the Mt Core 23 than the Mt Core 35 when comparing both pH 4 vs. pH 7 and pH 4 +Al vs. pH 7 treatments (Fig. 4.8A). The fold change in expression was similar for both Mt Core 23 and Mt Core 35 when pH 4+Al was compared to pH 4 treatment (Fig. 4.8B) suggesting that it is an Al-responsive gene although it may not be associated with an Al tolerance response.

The thioredoxin gene, coding for an antioxidant protein related to ROS (reactive oxygen species) scavenging mechanisms (Dos Santos and Rey, 2006), was found to be up-regulated under Al treatment in sensitive and tolerant *M. truncatula* plants (Chandran et al., 2008a). Similarly, the fold change in relative gene expression of the thioredoxin (Medtr2g007340) was higher in root tissues of the Mt Core 23 compared to Mt core 35 when pH 4 and pH 4+Al treatments were considered relative to pH 7, and a bigger fold change was detected at pH 4 relative to pH 7 (Fig. 4.9A). These results highlight the differential gene response of this gene to both acid and Al treatments. The same tendency was observed when comparing the relative gene expression between pH 4 +Al and pH 4 treatments (Fig. 4.9B). These results suggest that Mt Core 23 may have an enhanced ROS scavenging activities in roots that may help protect the roots from oxidative damage in addition to an organic acid exudation mechanism.

Peroxidases are oxi-reductases that use a variety of substrates as hydrogen donors in the presence of hydrogen peroxide. They play a role in ROS generation and also may be involved with the mechanisms of ROS scavenging (Chandran et al., 2008). Results from that study found that genes encoding peroxidases were up regulated in sensitive plants when exposed to Al. Three different peroxidase related gene sequences were targeted and evaluated in this study to identify variable gene expression profiles in roots vs. leaves supporting the dual role of this enzyme both in response to Al and acid responses. The transcript accumulation of the peroxidase (Medtr2g029800) was higher in root tissues for the Mt Core 35 than the Mt Core 23 when comparing pH 4 and pH 4 +Al treatments to pH 7 (Fig. 4.10A). The same patterns of gene expression were observed between pH 4 +Al and pH 4 treatments (Fig. 4.10B). Mt Core 23 showed a higher fold

change in relative gene expression between pH 4 and pH 7, as well as under pH 4 +Al and pH 7 in leaf tissue (4.11A). The relative fold change in relative gene expression between pH 4 +Al and pH 4 treatments was higher for Mt Core 35 (Fig. 4.11B). The changes in gene expression for the peroxidase gene (Medtr2g029830) between the root tissues of plants grown at pH 4 vs. pH 7, and pH 4 +Al vs. pH 7 were higher for Mt Core 23 than Mt Core 35 (Fig. 4.12A). However, the fold change in relative gene expression between pH 4 +Al and pH 4 was higher for Mt Core 35 (Fig. 4.12B). The same tendency was observed for the same peroxidase in leaf tissue (Fig. 4.13A and 4.13B).

References

- Anoop, V.M., U. Basu, M.T. McCammon, L. McAlister-Henn and G.J. Taylor. 2003. Modulation of citrate metabolism alters aluminum tolerance in yeast and transgenic canola overexpressing a mitochondrial citrate synthase. *Plant Physiology* 132:2205-2217. doi:10.1104/pp.103.023903.
- Barone, P., D. Rosellini, P. Lafayette, J. Bouton, F. Veronesi, and W. Parrott. 2008. Bacterial citrate synthase expression and soil aluminum tolerance in transgenic alfalfa. *Plant Cell R.* 27:893-901.
- Chandran D., N. Sharopova, K. VandenBosch, D.F. Garvin, and D.A. Samac. 2008a. Physiological and molecular characterization of aluminum resistance in *Medicago truncatula*. *BMC Plant Biology* 8:89.
- Chandran, D., N. Sharopova, S. Ivashuta, J. Gantt, K. Vandenbosch, and D. Samac. 2008b. Transcriptome profiling identified novel genes associated with aluminum

- toxicity, resistance and tolerance in *Medicago truncatula*. *Planta*, 228 (1):151-166.
- Han Y., Y. Kang, I. Torres-Jerez, F. Cheung, and C.D. Town. 2011. Genome-wide SNP discovery in tetraploid alfalfa using 454 sequencing and high-resolution melting analysis. *BMC Genomics* 12:350.
- Iuchi, S., H. Koyama, A. Iuchi, Y. Kobayashi, S. Kitabayashi, Y. Kobayashi, T. Ikka, T. Hirashama, K. Shinozaki, and M. Kobayashi. 2007. Zinc finger protein *STOP1* is critical for proton tolerance in *Arabidopsis* and co-regulates a key gene in aluminum tolerance. *Proc. Natl. Acad. Sci. USA* 104:9900-9905.
- Kakar K, M. Wandrey, T. Czechowski, T. Gaertner, W. R. Scheible, et al. 2008. A community resource for high-throughput quantitative RT-PCR analysis of transcription factor gene expression in *Medicago truncatula*. *Plant Methods* 4:18.
- Khu D.-M., R. Reyno, Y. Han, P.X. Zhao, J.H. Bouton, E.C. Brummer, and M.J. Monteros. 2013. Identification of aluminum tolerance quantitative trait loci in tetraploid alfalfa. *Crop Sci.* 53:148-163.
- Kochian L.V., M.A. Piñeros, and O.A. Hoekenga. 2005. The physiology, genetics and molecular biology of plant aluminum resistance and toxicity *Plant Soil*. 274:175-195.
- Li, X., A. Acharya, A.D. Farmer, J.A. Crow, A.K. Bharti, R.S. Kramer, Y. Wei, Y. Han, J. Gou, G.D. May, M.J. Monteros, and E.C. Brummer. 2012. Prevalence of single nucleotide polymorphism among 27 diverse alfalfa genotypes as assessed by transcriptome sequencing. *BMC Genomics* 13:568.

- Livak, K.J. and T.D. Schmittgen. 2001. Analysis of relative gene expression data using Real-Time Quantitative PCR and the $2^{-\Delta\Delta CT}$ method. *Methods* 25:402-408
doi:<http://dx.doi.org/10.1006/meth.2001.1262>.
- Landschütze V, B. Müller-Röber and L. Willmitzer. 1995. Mitochondrial citrate synthase from potato predominant expression in mature leaves and young flower buds. *Planta* 196:756-64.
- Ma, J.F. 2000. Role of organic acids in detoxification of aluminum in higher plants. *Plant and Cell Physiol* 41:383-390. doi:10.1093/pcp/41.4.383.
- Ma, J.F., P.R. Ryan and E. Delhaize. 2001. Aluminium tolerance in plants and the complexing role of organic acids. *Trends in Plant Science* 6:273-278.
doi:[http://dx.doi.org/10.1016/S1360-1385\(01\)01961-6](http://dx.doi.org/10.1016/S1360-1385(01)01961-6).
- Magalhaes, J.V. 2010. How a microbial drug transporter became essential for crop cultivation on acid soils: aluminium tolerance conferred by the multidrug and toxic compound extrusion (MATE) family. *Annals of Botany* 106: 199-203.
doi:10.1093/aob/mcq115.
- Pfaffl, M.W. 2001. A new mathematical model for relative quantification in real-time RT-PCR. *Nucleic Acids Research* 29:e45. doi:10.1093/nar/29.9.e45.
- Piñeros, M.A., J.E. Shaff, H.S. Manslank, V.M. Carvalho Alves and L.V. Kochian. 2005. Aluminum resistance in maize cannot be solely explained by root organic acid exudation. A comparative physiological study. *Plant Physiol* 137:231-241.
doi:10.1104/pp.104.047357.

- Ramakers C., J. M. Ruijter, R. H. Lekanne Deprez, A. F. M. Moorman. 2003. Assumption-free analysis of quantitative real-time polymerase chain reaction (PCR) data. *Neurosci. Lett.* 339:62-66.
- Rozen S. and H. Skaletsky. 1999, Primer3 on the WWW for general users and for biologist programmers. *Methods Mol Biol.* 132:365-86.
- Ryan, P., E. Delhaize and D. Jones. 2001. Function and mechanism of organic anion exudation from plant roots. *Annual Review of Plant Physiology and Plant Molecular Biology* 52:527-560. doi:doi:10.1146/annurev.arplant.52.1.527.
- Sasaki, T., Y. Yamamoto, B. Ezaki, M. Katsuhara, S.J. Ahn, P.R. Ryan, et al. 2004. A wheat gene encoding an aluminum-activated malate transporter. *The Plant Journal* 37:645-653. doi:10.1111/j.1365-313X.2003.01991.x.
- Udvardi M. K., Czechowski T. and WR. Scheible. 2008. Eleven golden rules of Quantitative RT-PCR. *Plant Cell* 20:1736-37.
- Vandesompele, J., K. De Preter, F. Pattyn, B. Poppe, N. Van Roy, A. De Paepe, and F. Speleman 2002. Accurate normalization of real-time quantitative RT-PCR data by geometric averaging of multiple internal control genes. *Genome Biology* 3: research0034.0031 - research0034.0011.
- Vieira Dos Santos, C. and P. Rey. 2006. Plant thioredoxins are key actors in the oxidative stress response. *Trends in Plant Science* 11:329-334. doi:http://dx.doi.org/10.1016/j.tplants.2006.05.005.

Table 4.1: Al response and tolerance candidate genes analyzed by qRT-PCR in the RIL population parental lines Mt Core 23 and Mt Core 35.

Transcript name	IMGAG annotation	Chromosome	Function
Malate dehydrogenase	Medtr2g045010	2	TCA cycle
Thioredoxin	Medtr2g007340	2	Reductase, scavenging of ROS
Peroxidase	Medtr2g029800	2	Oxi-reductase, generation and scavenging of ROS
Peroxidase	Medtr2g029830	2	Oxi-reductase, generation and scavenging of ROS
Citrate synthase	Medtr3g048920	3	Energy metabolism and TCA cycle
Citrate synthase	Medtr5g091930	5	Energy metabolism and TCA cycle
Citrate transporter	Medtr7g070210	7	Al activated organic acid transporter

Dehydrine	Medtr7g086340	7	Abiotic and/or biotic stress responses (cold acclimation)
Metal ion binding	Medtr7g100450	7	Heavy metal transport/detoxification
Citrate transporter	Medtr8g036660	8	Al activated organic acid transporter
Malate transporter	Medtr8g104120	8	Al activated organic acid transporter

Supplementary Table 4.1: Sequences for the forward (PF) and reverse (PR) primers targeting specific transcripts with the unique IMGAG annotations and utilized to evaluate the gene expression of Mt Core 23 and Mt Core 35 using qRT-PCR.

Transcript name	IMGAG annotation	Primer sequence
Dehydrine	Medtr7g086340	PF 5'-ACAAGGAGGGATTTGTTGACAAG-3' PR 5'-TCCTTCTTCTTTTTCTTTTCACCATCT-3'
Citrate synthase	Medtr5g091930	PF 5'-TCACCCGTGGCCAACCT-3' PR 5'-TTCTTGCCGGTTCTCTCATCA-3'
Citrate synthase	Medtr3g048920	PF 5'-TGCACATCCTATGGGTGTACTTG-3' PR 5'-TGCATCGGGATGAAAAACAG-3'
Malate dehydrogenase	Medtr2g045010	PF 5'-AGAAAGCTATAGTGCACGGGAAA-3' PR 5'-AGTCCAATGTAGCCCCAAAGC-3'
Citrate transporter	Medtr8g036660	PF 5'-TTTTTGCTGATGGTTTGGCTATAG-3' PR 5'-TGTTACAGTCTTTCTCCGCGAAA-3'
Citrate transporter	Medtr7g070210	PF 5'-CATGGCGTTGCGTGTCTAG-3' PR 5'-TCCCATGGACCACTTTTGCT-3'
Malate transporter	Medtr8g104120	5'-TGAAGAATTGGGTGAGAAAGCTAA-3' 5'-GCCACCGCGCCTTGT-3'
Metal ion binding	Medtr7g100450	PF 5'-ACTGTCACTGCTCCTAGTTCACCTT-3' PR 5'-TGGCCTTTTCATGGACATGTT-3'
Thioredoxin	Medtr2g007340	PF 5'-GGTTGATGTGCAAGTGAGAGAGTT-3'

		PR 5'-GGGAGAATGCAGTCAGAATGG-3'
Peroxidase	Medtr2g029800	PF 5'-CCGGCTCCATTCAATTCG-3' PR 5'-TGAGGCCTTGAGCAGCAAAT-3'
Peroxidase	Medtr2g029830	5'-CGCACAATATGTCCCAATGG-3' 5'-GAGTCGTTGGATCGAAATTGGT-3'

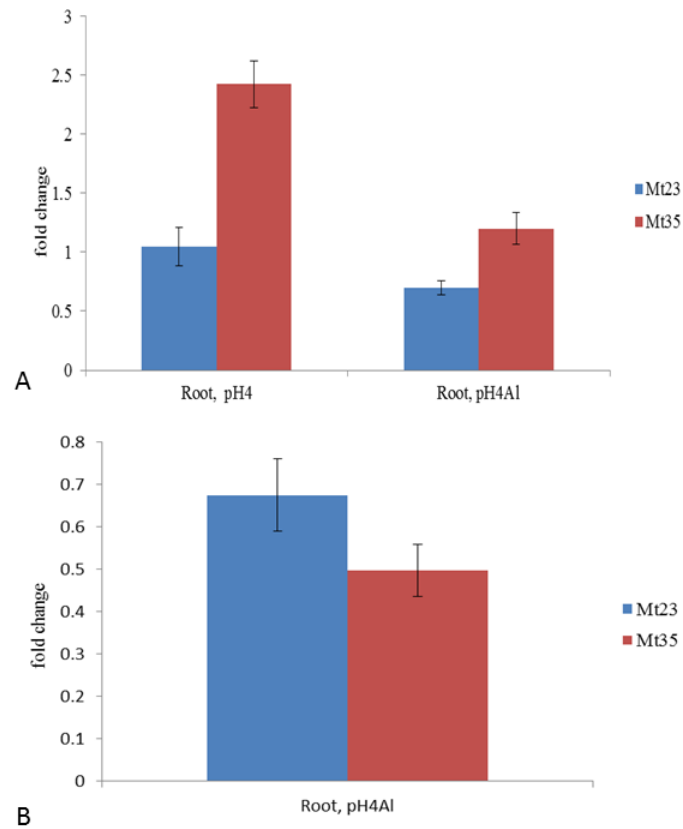


Figure 4.1: Relative gene expression (fold change) of the dehydrine gene (Medtr7g086340) in root tissues of Mt Core 23 and Mt Core 35. A) Gene expression of the dehydrine gene at pH 4 and pH 4+ Al relative to pH 7, B) Gene expression of the dehydrine gene at pH 4+ Al 20 μ M relative to pH 4.

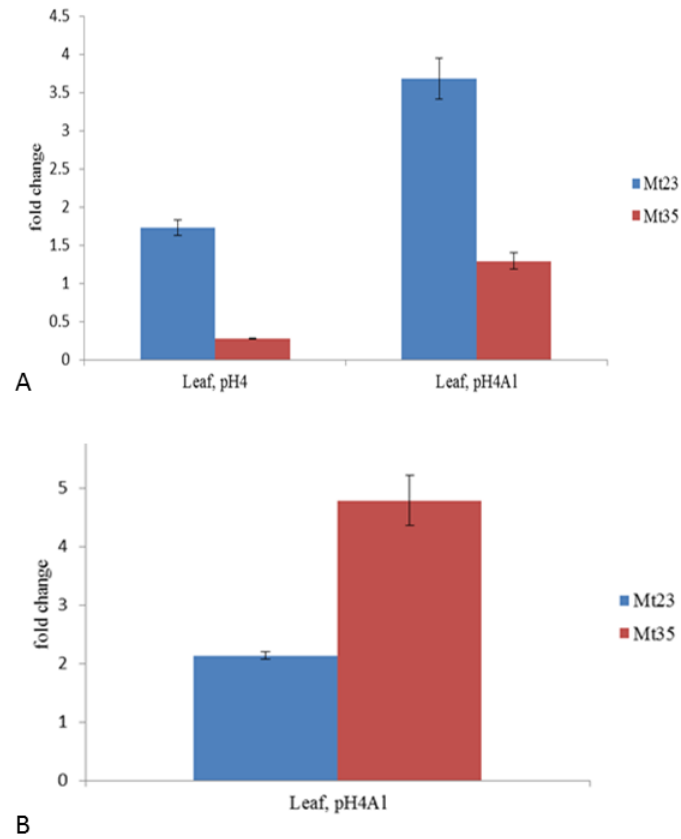


Figure 4.2: Relative gene expression (fold change) of the dehydrine gene (Medtr7g086340) in leaf tissues of Mt Core 23 and Mt Core 35. A) Gene expression of the dehydrine gene at pH 4 and pH 4+Al 20 μ M relative to pH 7, B) Gene expression of the dehydrine gene at pH 4+ Al 20 μ M relative to pH 4.

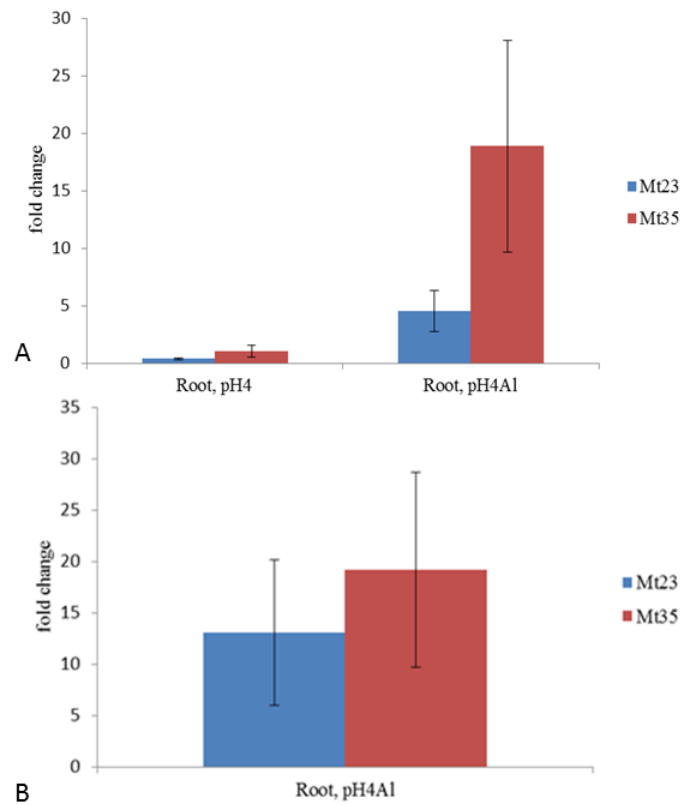


Figure 4.3: Relative gene expression (fold change) of the citrate synthase gene (Medtr5g091930) in root tissues of Mt Core 23 and Mt Core 35. A) Gene expression of the citrate synthase gene at pH 4 and pH 4+Al 20 μM relative to pH 7, B) Gene expression of the citrate synthase gene at pH 4+ Al 20 μM relative to pH 4.

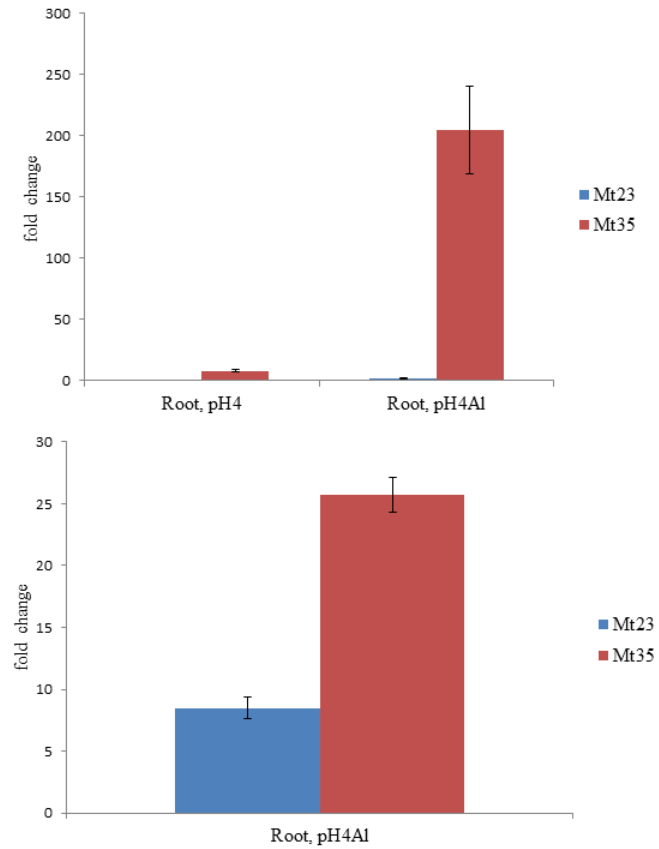


Figure 4.4: Relative gene expression (fold change) of the citrate synthase gene (Medtr3g048920) in root tissues of Mt Core 23 and Mt Core 35. A) Gene expression of the citrate synthase gene at pH 4 and pH 4+Al 20 μM relative to pH 7, B) Gene expression of the citrate synthase gene at pH 4+ Al 20 μM relative to pH 4.

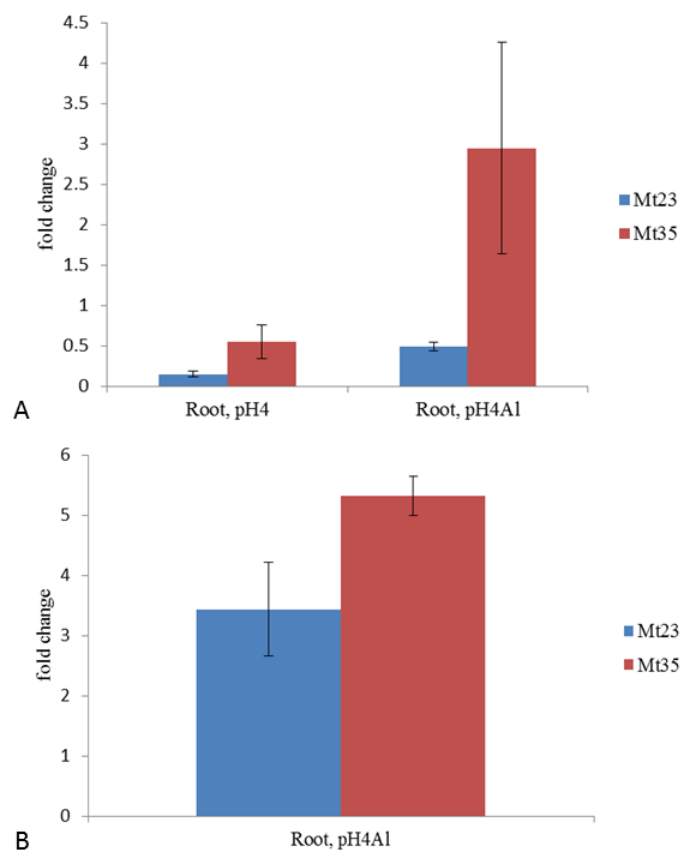


Figure 4.5: Relative gene expression (fold change) of the malate dehydrogenase gene (Medtr2g045010) in root tissues of Mt Core 23 and Mt Core 35. A) gene expression of the malate dehydrogenase gene at pH 4 and pH 4+Al 20 μ M relative to pH 7, B) Gene expression of the malate dehydrogenase gene at pH 4+ Al 20 μ M relative to pH 4.

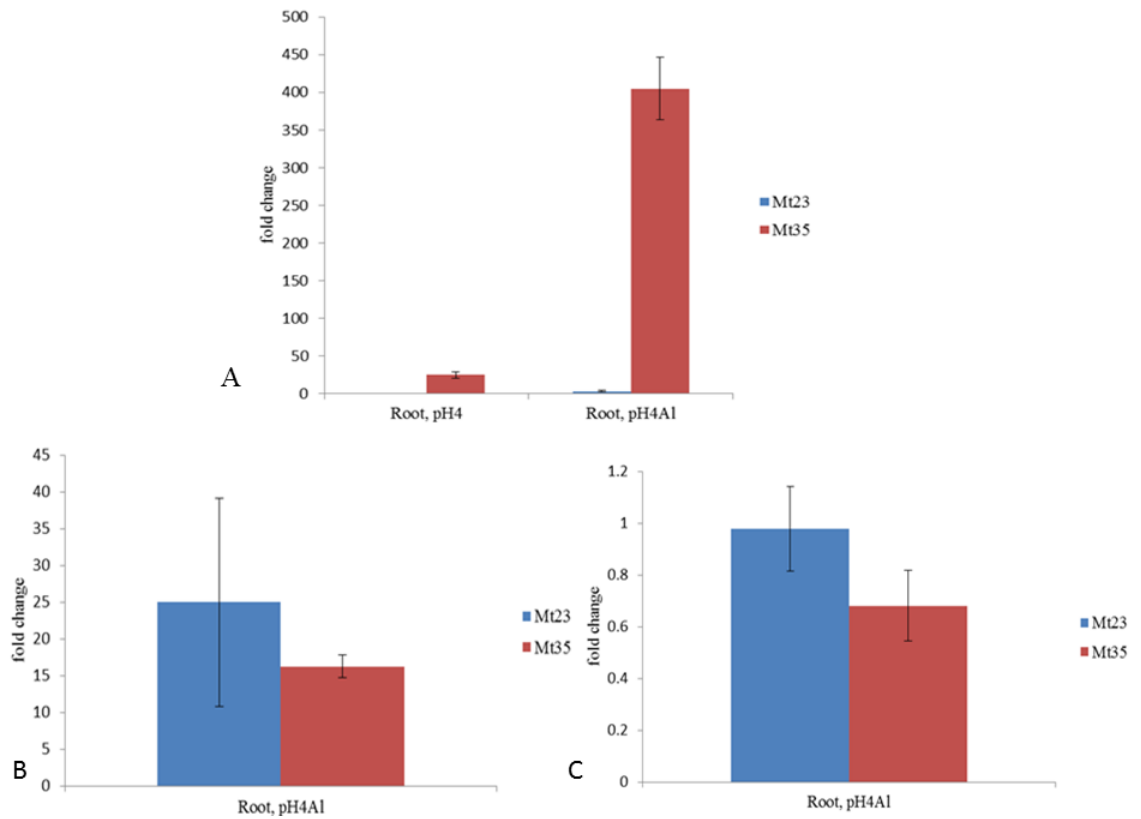


Figure 4.6: Relative gene expression (fold change) of the citrate transporter gene (Medtr8g036660) in root tissues of Mt Core 23 and Mt Core 35. A) Gene expression of the citrate transporter gene at pH 4 and pH 4+ Al 20 μM relative to pH 7, B) Gene expression of the citrate transporter gene at pH 4+ Al 20 μM relative to pH 4, C) Gene expression of the citrate transporter gene (Medtr7g070210) at pH 4+ Al 20 μM relative to pH 4.

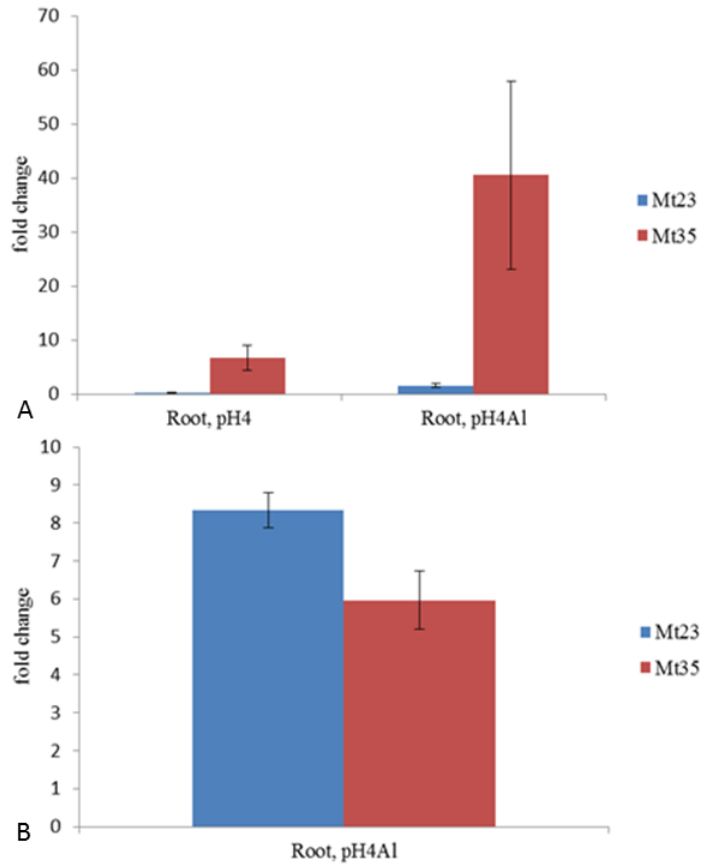


Figure 4.7: Relative gene expression (fold change) of the malate transporter gen (Medtr8g104120) in root tissues of Mt Core 23 and Mt Core 35. A) Gene expression of the malate transporter gene at pH 4 and pH 4+Al 20 μM relative to pH 7, B) Gene expression of the malate transporter gene at pH 4+ Al 20 μM relative to pH 4.

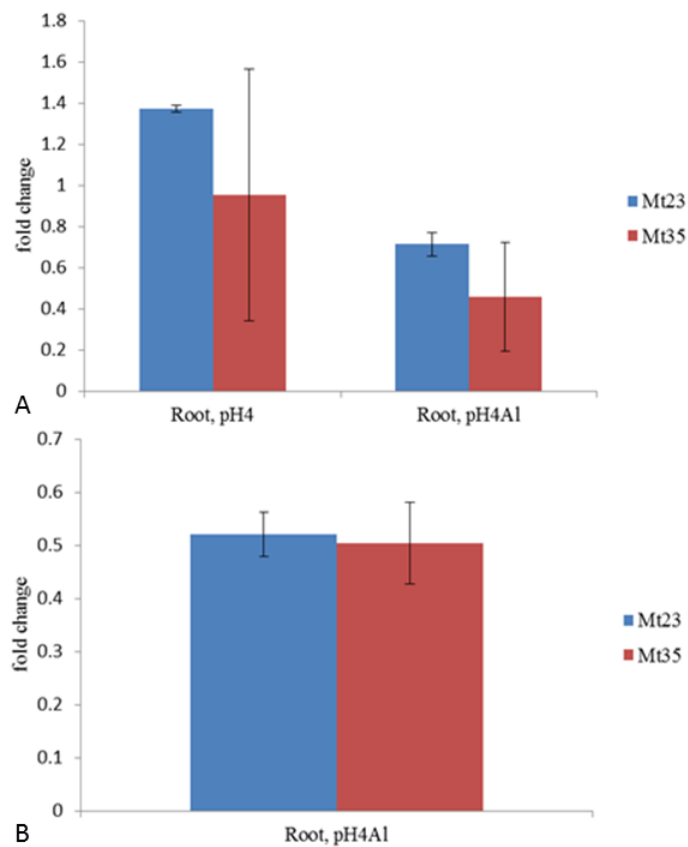


Figure 4.8: Relative gene expression (fold change) of the metal ion binding protein gene (Medtr7g100450) in root tissues of Mt Core 23 and Mt Core 35. A) Gene expression of the metal ion binding protein gene at pH 4 and pH 4+ Al 20 μM relative to pH 7, B) Gene expression of the metal ion binding protein gene at pH 4+ Al 20 μM relative to pH 4.

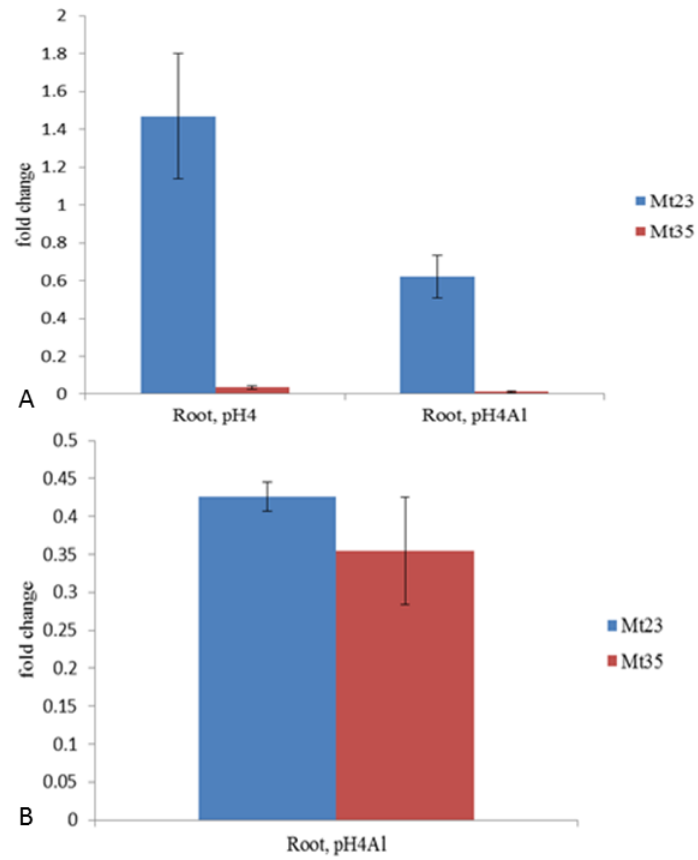


Figure 4.9: Relative gene expression (fold change) of the thioredoxin gene (Medtr2g007340) in root tissues of Mt Core 23 and Mt Core 35. A) Gene expression of the thioredoxin gene at pH 4 and pH 4+ Al 20 μ M relative to pH 7, B) Gene expression of the thioredoxin gene at pH 4+ Al 20 μ M relative to pH 4.

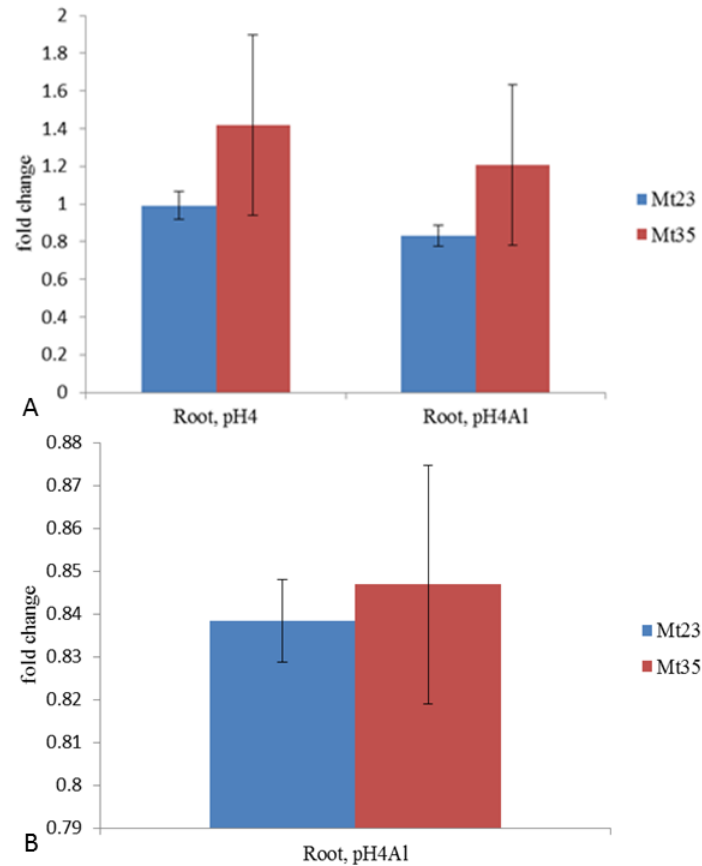


Figure 4.10: Relative gene expression (fold change) of the peroxidase gene (Medtr2g029800) in root tissues of Mt Core 23 and Mt Core 35 A) Gene expression of the peroxidase gene at pH 4 and pH 4+ Al 20 μ M relative to pH 7, B) Gene expression of the peroxidase gene at pH 4+ Al 20 μ M relative to pH 4.

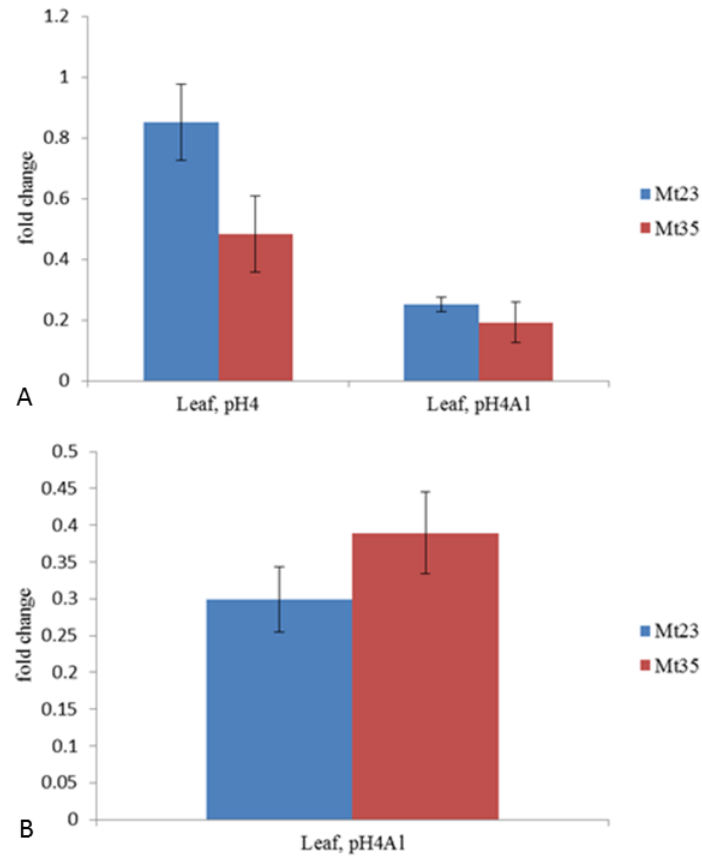


Figure 4.11: Relative gene expression (fold change) of the peroxidase gene (Medtr2g029800) in leaf tissues of Mt Core 23 and Mt Core 35. A) Gene expression of the peroxidase gene at pH 4 and pH 4+Al 20 μ M relative to pH 7, B) Gene expression of the peroxidase gene at pH 4+ Al 20 μ M relative to pH 4.

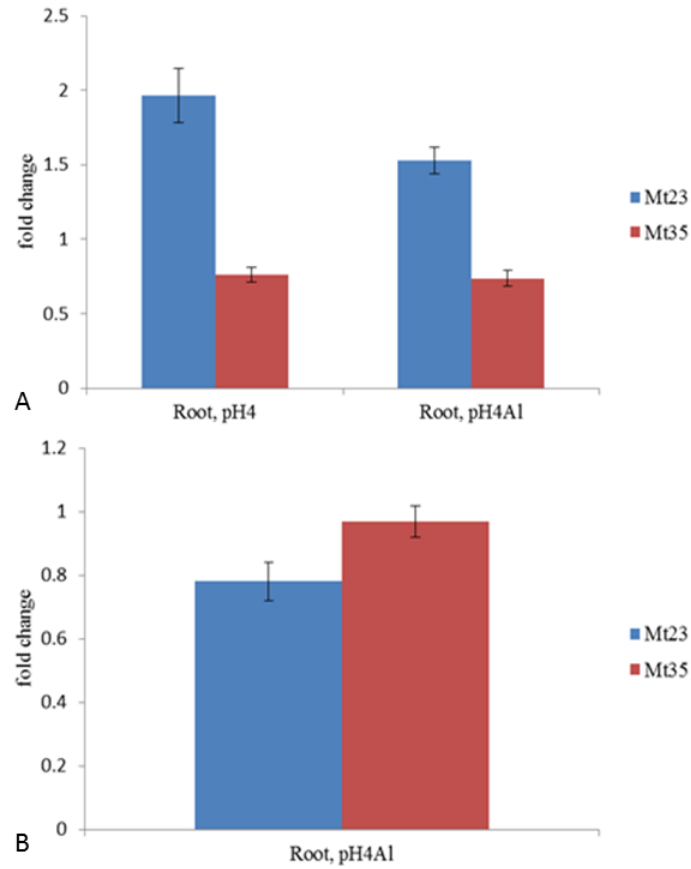


Figure 4.12: Relative gene expression (fold change) of the peroxidase gene (Medtr2g029800) in root tissues of Mt Core 23 and Mt Core 35. A) Gene expression of the peroxidase gene at pH 4 and pH 4+Al 20 μ M relative to pH 7, B) Gene expression of the peroxidase gene at pH 4+ Al 20 μ M relative to pH 4.

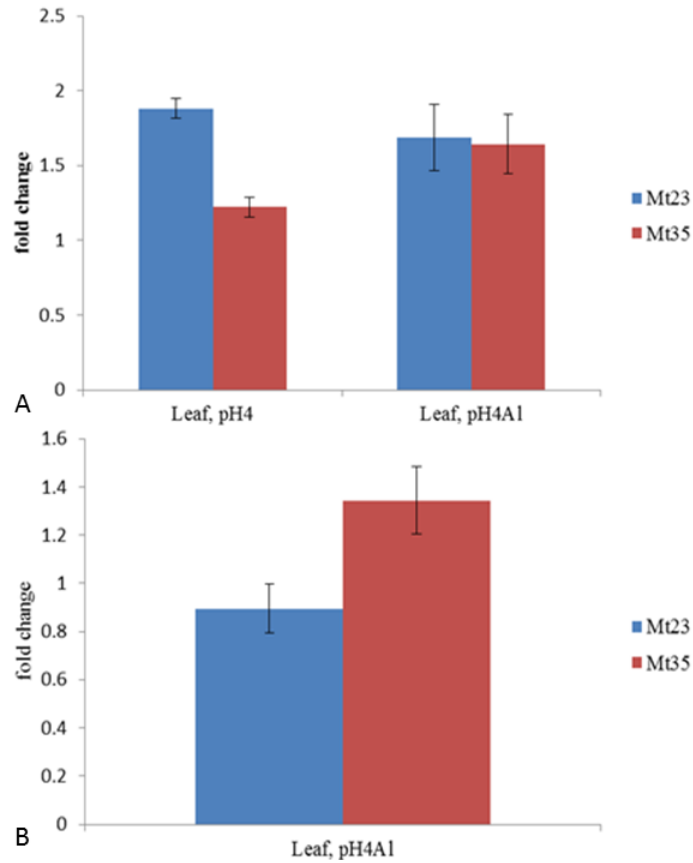


Figure 4.13: Relative gene expression (fold change) of the peroxidase gene (Medtr2g029830) in leaf tissues of Mt Core 23 and Mt Core 35. A) Gene expression of the peroxidase gene at pH 4 and pH 4+Al 20 μ M relative to pH 7, B) Gene expression of the peroxidase gene at pH 4+ Al 20 μ M relative to pH 4.

CHAPTER 5

CONCLUSION

A considerable portion of the total arable soil in the world is acidic. Although the low fertility of acid soils is due to a combination of mineral deficiencies and toxicities, toxicity due to aluminum (Al) is the main factor limiting crop production in most acid soils. The addition of lime to acid soils is an approach that could ameliorate these types of soil toxicities although the process is expensive and not always efficient. Therefore, strategies aimed at identifying genetic mechanisms of aluminum tolerance for deployment in crop breeding programs are relevant and critically needed in economical important forage crops. One strategy to increase our understanding of Al tolerance mechanisms that could address this issue in legumes is through translational genomics approaches leveraging knowledge from the model species *Medicago truncatula*. Due to the various mechanisms of Al tolerance in plants and their sometimes complex inheritance patterns, understanding the specific mechanisms and responses relevant to the target crop legume species with diminished productivity due to acid soils syndrome is critical.

This study resulted in the identification of putative genomic regions associated with responses to acid and Al in a *M. truncatula* RIL population derived from the cross between the Al tolerant Mt Core 23 and the Al sensitive Mt Core 35. These genomic regions were located on LG 2 (which corresponds with chromosome 2 of *M. truncatula*), LG 3 (which corresponds to chromosome 3 of *M. truncatula*), and LG 5 (which

corresponds to chromosome 7 of *M. truncatula*). The genomic regions were associated with the root length (RL) traits at pH 4, RL at pH 4 +Al 20 μ M, RL at pH 4/ RL at pH 7, RL at pH 4 +Al 20 μ M/ RL at pH 7 and RL at pH 4 +Al 20 μ M/ RL at pH 4. The strategies for SNP genotyping included a hybrid approach between using Illumina's Golden Gate array for *M. truncatula* complemented by SNP genotyping of target Al-responsive genes using the HRM approach. Root length measurements obtained from evaluations in the WPA in media for acid and Al growth responses were able to distinguish phenotypic differences between the parental lines and the resulting RIL population. Therefore, the combination of phenotypic evaluations with the SNP genotyping strategies was successful to identify genomic regions associated with acid and Al tolerance mechanisms in *M. truncatula*.

The identification of molecular markers in specific genomic regions and targeting key Al-responsive genes enabled us to predict the phenotypes of a validation set of RIL lines with markers flanking acid and Al tolerance associated genomic regions. The frequency of successful phenotype prediction particularly for the top performers with the molecular markers highlights the value of mapping studies to identify molecular markers for practical selection approaches.

The candidate genes evaluated for differential expression between the parental genotypes in response to Al were either responsive to Al from previous studies, located on chromosomes 2, 3 and 7 of *M. truncatula* near the QTL intervals or both. The results from the gene expression profiling between the Mt Core 23 and Mt Core 35 further support the identification of QTLs for Al tolerance with small effects detected on chromosomes 2, 3 and 7 of the *M. truncatula*.

The outcomes of this research serve to further understand mechanisms underlying acid and Al tolerance in *M. truncatula* and further inform approaches for practical crop improvement in the closely related legume alfalfa. Ongoing work includes genotyping of the RIL population using genotype by sequencing (GBS) to enhance marker coverage on all eight chromosomes to facilitate identification of additional Al tolerance QTLs. Further studies in gene expression to dissect genes expressed as a response to the initial exposure to Al vs. those involved in a sustained response to growth under acid and Al toxic conditions could be valuable for practical crop improvement strategies. Further quantification of Al accumulation in plant tissues would also provide insights on the relative contributions of Al exclusion via organic acid secretion vs. Al sequestration. Overall, the outcomes of the completed and proposed research activities has value for increasing the knowledge of abiotic stress responses as well as for future practical plant breeding applications.